

## 1 JGI Plant Gene Atlas: An updateable transcriptome resource to improve structural 2 annotations and functional gene descriptions across the plant kingdom

3  
4 Avinash Sreedasyam<sup>1\*</sup>, Christopher Plott<sup>1</sup>, Md Shakhawat Hossain<sup>2#<sup>a</sup></sup>, John T. Lovell<sup>1,3</sup>, Jane Grimwood<sup>1</sup>,  
5 Jerry W. Jenkins<sup>1</sup>, Christopher Daum<sup>3</sup>, Kerrie Barry<sup>3</sup>, Joseph Carlson<sup>3</sup>, Shengqiang Shu<sup>3</sup>, Jeremy Phillips<sup>3</sup>,  
6 Mojgan Amirebrahimi<sup>3</sup>, Matthew Zane<sup>3</sup>, Mei Wang<sup>3</sup>, David Goodstein<sup>3</sup>, Fabian B. Haas<sup>4#<sup>b</sup></sup>, Manuel Hiss<sup>4#<sup>c</sup></sup>,  
7 Pierre-François Perroud<sup>4#<sup>d</sup></sup>, Sara S. Jawdy<sup>5</sup>, Rongbin Hu<sup>5</sup>, Jenifer Johnson<sup>3</sup>, Janette Kropat<sup>6</sup>, Sean D.  
8 Gallaher<sup>6#<sup>e</sup></sup>, Anna Lipzen<sup>3</sup>, Ryan Tillman<sup>1</sup>, Eugene V. Shakirov<sup>7#<sup>f</sup></sup>, Xiaoyu Weng<sup>7</sup>, Ivone Torres-Jerez<sup>8</sup>, Brock  
9 Weers<sup>9</sup>, Daniel Conde<sup>10</sup>, Marilia R. Pappas<sup>11</sup>, Lifeng Liu<sup>3</sup>, Andrew Muchlinski<sup>12#<sup>g</sup></sup>, Hui Jiang<sup>13</sup>, Christine  
10 Shyu<sup>13#<sup>h</sup></sup>, Pu Huang<sup>13#<sup>i</sup></sup>, Jose Sebastian<sup>13#<sup>j</sup></sup>, Carol Laiben<sup>13#<sup>k</sup></sup>, Alyssa Medlin<sup>13#<sup>l</sup></sup>, Sankalpi Carey<sup>13#<sup>m</sup></sup>, Alyssa A.  
11 Carrell<sup>14</sup>, Mariano Perales<sup>10,15</sup>, Kankshita Swaminathan<sup>1</sup>, Isabel Allona<sup>10,15</sup>, Dario Grattapaglia<sup>11</sup>, Elizabeth  
12 A. Cooper<sup>16#<sup>n</sup></sup>, Dorothea Tholl<sup>12</sup>, John P. Vogel<sup>3</sup>, David J Weston<sup>14</sup>, Xiaohan Yang<sup>5</sup>, Thomas P. Brutnell<sup>17</sup>,  
13 Elizabeth A. Kellogg<sup>13</sup>, Ivan Baxter<sup>13</sup>, Michael Udvardi<sup>8#<sup>o</sup></sup>, Yuhong Tang<sup>8</sup>, Todd C. Mockler<sup>13</sup>, Thomas E.  
14 Juenger<sup>7</sup>, John Mullet<sup>9</sup>, Stefan A. Rensing<sup>4#<sup>p</sup></sup>, Gerald A. Tuskan<sup>5</sup>, Sabeeha S. Merchant<sup>6#<sup>q</sup></sup>, Gary Stacey<sup>2</sup>,  
15 Jeremy Schmutz<sup>1,3\*</sup>

16  
17 <sup>1</sup> HudsonAlpha Institute for Biotechnology, Huntsville, AL, USA

18 <sup>2</sup> Divisions of Plant Science and Biochemistry, National Center for Soybean Biotechnology, University of Missouri, Columbia,  
19 MO, USA

20 <sup>3</sup> Joint Genome Institute, Lawrence Berkeley National Laboratory, Berkeley, CA, USA

21 <sup>4</sup> Plant Cell Biology, Faculty of Biology, University of Marburg, Karl-von-Frisch-Str, Marburg, Germany

22 <sup>5</sup> Center for Bioenergy Innovation, Oak Ridge National Laboratory, Oak Ridge, TN, USA

23 <sup>6</sup> Department of Chemistry and Biochemistry and Institute for Genomics and Proteomics, University of California, Los Angeles,  
24 CA, USA

25 <sup>7</sup> Department of Integrative Biology, University of Texas at Austin, Austin, TX, USA

26 <sup>8</sup> Noble Research Institute, Ardmore, OK, USA

27 <sup>9</sup> Department of Biochemistry and Biophysics, Texas A&M University, College Station, TX, USA

28 <sup>10</sup> Centro de Biotecnología y Genómica de Plantas, Universidad Politécnica de Madrid, Instituto Nacional de Investigación y  
29 Tecnología Agraria y Alimentaria (INIA-CSIC), Madrid, Spain

30 <sup>11</sup> Laboratório de Genética Vegetal, EMBRAPA Recursos Genéticos e Biotecnologia, EPQB Final W5 Norte, Brasília, Brazil

31 <sup>12</sup> Department of Biological Sciences, Virginia Tech, Blacksburg, VA, USA

32 <sup>13</sup> Donald Danforth Plant Science Center, St. Louis, MO, USA

33 <sup>14</sup> Biosciences Division, Oak Ridge National Laboratory, Oak Ridge, TN, USA

34 <sup>15</sup> Departamento de Biotecnología-Biología Vegetal, Escuela Técnica Superior de Ingeniería Agronómica, Alimentaria y de  
35 Biosistemas, Universidad Politécnica de Madrid, Madrid, Spain

36 <sup>16</sup> Advanced Plant Technology Program, Clemson University, Clemson, SC, USA

37 <sup>17</sup> Gateway Biotechnology Inc, St. Louis, MO, USA

38  
39 \*Corresponding authors, email: [asreedasyam@hudsonalpha.org](mailto:asreedasyam@hudsonalpha.org), [jschmutz@hudsonalpha.org](mailto:jschmutz@hudsonalpha.org)

40  
41 <sup>#a</sup> Current address: Texas A&M AgriLife Research and Department of Soil and Crop Sciences, Texas A&M University, College  
42 Station, TX, USA

43 <sup>#b</sup> Current address: Department of Algal Development and Evolution, Max Planck Institute for Biology Tübingen, Tübingen,  
44 Germany

45 <sup>#c</sup> Current address: GSK Vaccines GmbH, Emil-von-Behring-Str, Marburg, Germany

46 <sup>#d</sup> Current address: Université Paris-Saclay, INRAE, AgroParisTech, Institut Jean-Pierre Bourgin (IJPB) Versailles, France

47 <sup>#e</sup> Current address: Department of Plant and Microbial Biology and Department of Molecular and Cell Biology, QB3,  
48 University of California, Berkeley, Berkeley, CA, USA

49 <sup>#f</sup> Current address: Department of Biological Sciences, Marshall University, Huntington, WV, USA

50 <sup>#g</sup> Current address: Firmaenich, San Diego, CA, USA

51 <sup>#h</sup> Current address: Bayer Crop Science, St. Louis, MO, USA

52 <sup>#i</sup> Current address: BASF Corporation, Durham, NC, USA

53 <sup>#j</sup> Current address: Department of Biological Sciences, Indian Institute of Science Education and Research, Berhampur (IISER)  
54 BPR, Odisha, India

55 <sup>#k</sup> Current address: Propper Asset Management, 17 Research Park Drive, St. Charles, MO, USA

56 <sup>#l</sup> Current address: Saginaw High School, 800 N Blue Mound Rd, Saginaw, TX, USA

57 <sup>#m</sup> Current address: Invitae Corporation, 1400 16th Street, San Francisco, CA, USA

58 <sup>#n</sup> Current address: Department of Bioinformatics and Genomics, University of North Carolina at Charlotte, Charlotte, NC, USA

59 <sup>#o</sup> Current address: Center for Crop Science, The University of Queensland, St. Lucia, Brisbane, Australia

60 <sup>#p</sup> Current address: Faculty of Chemistry and Pharmacy, University of Freiburg, Freiburg, Germany

61 <sup>#q</sup> Environmental Genomics and Systems Biology, Lawrence Berkeley National Laboratory, Berkeley, CA, USA

62  
63

64

## 65 ABSTRACT

66 Gene functional descriptions, which are typically derived from sequence similarity to experimentally validated  
67 genes in a handful of model species, offer a crucial line of evidence when searching for candidate genes that  
68 underlie trait variation. Plant responses to environmental cues, including gene expression regulatory variation,  
69 represent important resources for understanding gene function and crucial targets for plant improvement  
70 through gene editing and other biotechnologies. However, even after years of effort and numerous large-scale  
71 functional characterization studies, biological roles of large proportions of protein coding genes across the plant  
72 phylogeny are poorly annotated. Here we describe the Joint Genome Institute (JGI) Plant Gene Atlas, a public  
73 and updateable data resource consisting of transcript abundance assays from 2,090 samples derived from 604  
74 tissues or conditions across 18 diverse species. We integrated across these diverse conditions and genotypes  
75 by analyzing expression profiles, building gene clusters that exhibited tissue/condition specific expression, and  
76 testing for transcriptional modulation in response to environmental queues. For example, we discovered  
77 extensive phylogenetically constrained and condition-specific expression profiles across many gene families  
78 and genes without any functional annotation. Such conserved expression patterns and other tightly co-  
79 expressed gene clusters let us assign expression derived functional descriptions to 64,620 genes with  
80 otherwise unknown functions. The ever-expanding Gene Atlas resource is available at JGI Plant Gene Atlas  
81 (<https://plantgeneatlas.jgi.doe.gov>) and Phytozome (<https://phytozome-next.jgi.doe.gov>), providing bulk access  
82 to data and user-specified queries of gene sets. Combined, these web interfaces let users access differentially  
83 expressed genes, track orthologs across the Gene Atlas plants, graphically represent co-expressed genes, and  
84 visualize gene ontology and pathway enrichments.

## 85 INTRODUCTION

86 The flowering plant, *Arabidopsis thaliana*, has served as a model for functional genomics over the past two  
87 decades. While the goal of functionally characterizing each *A. thaliana* gene by the year 2010 (Koornneef and  
88 Meinke 2010) has yet to be fully realized, many large-scale studies, such as gene knock-out collections for  
89 reverse genetics, have tested the phenotypic effects nearly half of *A. thaliana* protein-coding genes (Berardini et  
90 al. 2015). These experimentally validated loci, and a massive set of predicted and curated gene functions form  
91 the foundation for gene characterization across 400M years of plant evolution.

92 Despite the potential for homology-based functional annotations across plants, putative gene functions in non-  
93 model plants are sparse, often containing a majority of genes with no functional descriptions. These knowledge  
94 gaps are undoubtedly due to the phylogenetic and functional scale of plant diversity. At one extreme, DNA or  
95 protein sequences may have diverged so that no genes have obvious *A. thaliana* homologs. However, even with  
96 homology, assigning gene function to distantly related plants assumes function is evolutionarily conserved. This  
97 assumption is clearly violated in many situations: flowering plants have evolved diverse adaptive traits,  
98 specialized organs/tissues, and environmental responses, all of which are poorly captured by a single model  
99 organism. Further, gene neofunctionalization, subfunctionalization and gene cooption may invalidate direct  
100 superimposition of gene annotation from one species to another (C. Li et al. 2012; Nicotra et al. 2010; Raissig et  
101 al. 2017). The addition of other model species, including *Brachypodium distachyon*, *Oryza sativa*, and  
102 *Physcomitrium patens*, has helped fill gaps in homology-based functional annotations. However, 16.1-56.9% ( $M$   
103 = 27.8;  $SD$  = 10.06) of protein coding genes across the plant phylogeny remain poorly characterized  
104 (**Supplemental Fig. 1**) (Gollery et al. 2006, 2007; Rhee and Mutwil 2014).

105 Incomplete gene functional annotations are not only due to an overreliance on few genetic model organisms,  
106 but also an inability to link experimental evidence across species. However, centralized functional databases  
107 containing information generated from new experiments such as ongoing large-scale transcriptome projects  
108 and genome-wide association studies could accelerate gene function discovery. Even with a central repository,  
109 interpretation and integration across diverse studies is difficult because experimental and analytical protocols  
110 are rarely standardized. For example, different sample collection, RNA isolation, library construction protocols,  
111 and sequencing platforms can result in significant variation in sequence coverage and estimates of gene  
112 expression (Levin et al. 2010; Ross et al. 2013; Sudmant, Alexis, and Burge 2015; Yu et al. 2014). This among-  
113 experiment variation reduces the accuracy and precision of comparisons across species and studies, which  
114 directly limits putative gene function inference from transcript abundance profiles.

115 Here, we present an updateable large-scale dataset and a suite of experimental protocols to facilitate functional  
116 gene prediction across the diversity of plants. Crucially, we have developed experimental conditions, tissue  
117 types, and analytical protocols that permit comprehensive analysis of gene expression across plants. We  
118 applied these conditions and collected 2,090 tissue samples from 18 plant species spanning single-celled

120 algae, bryophytes, and flowering plants. This integrated dataset (1) forms a foundation to improve gene  
121 functional annotations, (2) facilitates cross-species comparative transcriptomics within controlled environmental  
122 and laboratory conditions, and (3) permits high-powered tests of gene regulatory evolution across  
123 phylogenetically diverse plant genomes. To demonstrate this functionality, we cataloged the expression profiles  
124 of annotated genes, and built co-expressed clusters of genes that exhibited tissue/condition specific  
125 expression patterns including responses to changes in nitrogen (N) regimes, abiotic stressors, and  
126 developmental stages. We systematically assigned expression derived functional descriptions to an average of  
127 40.6% ( $SD = 12.6$ ) of annotated genes in the assessed genomes, 9.5% of which previously had no known  
128 function. This substantial transcriptomic resource is available to the research community at JGI Plant Gene  
129 Atlas (<https://plantgeneatlas.jgi.doe.gov>) and through Phytozome, the JGI Plant Portal, at [https://phytozome-](https://phytozome-next.jgi.doe.gov)  
130 [next.jgi.doe.gov](https://phytozome-next.jgi.doe.gov) (Goodstein et al. 2012).

131

## 132 SCOPE OF DATA GENERATED

133 We developed the JGI Gene Atlas from 15.4 trillion sequenced RNA bases (Tb) and 2,090 RNA-seq samples  
134 across 9 JGI plant flagship genomes and 9 other reference plants (**Table 1**). For each of the sequenced plants,  
135 we collected tissue samples representing appropriate developmental stages, growth conditions, tissues, and  
136 abiotic stresses (**Fig. 1**). To reduce residual environmental variance, we followed standard growth conditions  
137 including light quality, quantity and duration, temperature, water, growth media, and nutrients. Experimental  
138 treatments were applied using standardized methods across all species (see Methods).

139

140 **Table 1 | JGI Plant Gene Atlas species.** Genome annotation versions of 18 diverse plants included in the current release.  
141

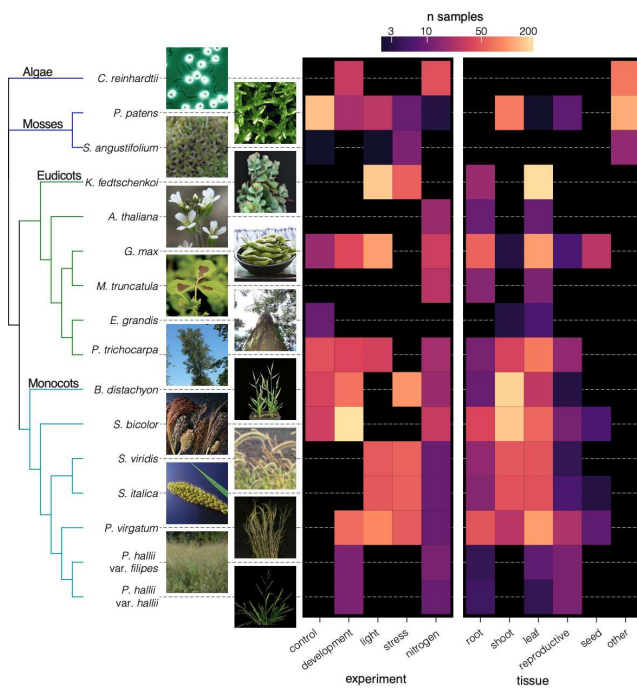
Genome	Version	Project	Taxonomy ID	Source
<i>Arabidopsis thaliana</i>	TAIR10	Gene Atlas	3702	<a href="https://phytozome-next.jgi.doe.gov/info/Athaliana_TAIR10">phytozome-next.jgi.doe.gov/info/Athaliana_TAIR10</a>
<i>Brachypodium distachyon</i>	v3.1	Gene Atlas	5143	<a href="https://phytozome-next.jgi.doe.gov/info/Bdistachyon_v3_1">phytozome-next.jgi.doe.gov/info/Bdistachyon_v3_1</a>
<i>Chlamydomonas reinhardtii</i>	v5.6	Gene Atlas	3055	<a href="https://phytozome-next.jgi.doe.gov/info/Creinhardtii_v5_6">phytozome-next.jgi.doe.gov/info/Creinhardtii_v5_6</a>
<i>Eucalyptus grandis</i>	v2.0	Gene Atlas	71139	<a href="https://phytozome-next.jgi.doe.gov/info/Egrandis_v2_0">phytozome-next.jgi.doe.gov/info/Egrandis_v2_0</a>
<i>Glycine max</i>	Wm82.a4.v1	Gene Atlas	3847	<a href="https://phytozome-next.jgi.doe.gov/info/Gmax_Wm82_a4_v1">phytozome-next.jgi.doe.gov/info/Gmax_Wm82_a4_v1</a>
<i>Kalanchoë fedtschenkoi</i>	v1.1	Gene Atlas	63787	<a href="https://phytozome-next.jgi.doe.gov/info/Kfedtschenkoi_v1_1">phytozome-next.jgi.doe.gov/info/Kfedtschenkoi_v1_1</a>
<i>Lupinus albus</i>	v1.1	Non-JGI	3870	<a href="https://phytozome-next.jgi.doe.gov/info/Lalbus_v1">phytozome-next.jgi.doe.gov/info/Lalbus_v1</a>
<i>Medicago truncatula</i>	Mt4.0v1	Gene Atlas	3880	<a href="https://phytozome-next.jgi.doe.gov/info/Mtruncatula_Mt4_0v1">phytozome-next.jgi.doe.gov/info/Mtruncatula_Mt4_0v1</a>
<i>Panicum hallii</i> var. <i>filipes</i>	v3.1	Gene Atlas	907226	<a href="https://phytozome-next.jgi.doe.gov/info/Phallii_v3_1">phytozome-next.jgi.doe.gov/info/Phallii_v3_1</a>
<i>Panicum hallii</i> var. <i>hallii</i>	v2.1	Gene Atlas	1504633	<a href="https://phytozome-next.jgi.doe.gov/info/PhalliiHAL_v2_1">phytozome-next.jgi.doe.gov/info/PhalliiHAL_v2_1</a>
<i>Physcomitrium patens</i>	v3.3	Gene Atlas	3218	<a href="https://phytozome-next.jgi.doe.gov/info/Ppatens_v3_3">phytozome-next.jgi.doe.gov/info/Ppatens_v3_3</a>
<i>Populus trichocarpa</i>	v4.1	Gene Atlas	3694	<a href="https://phytozome-next.jgi.doe.gov/info/Ptrichocarpa_v4_1">phytozome-next.jgi.doe.gov/info/Ptrichocarpa_v4_1</a>
<i>Panicum virgatum</i>	v5.1	Gene Atlas	38727	<a href="https://phytozome-next.jgi.doe.gov/info/Pvirgatum_v5_1">phytozome-next.jgi.doe.gov/info/Pvirgatum_v5_1</a>
<i>Sorghum bicolor</i>	v3.1.1	Gene Atlas	4558	<a href="https://phytozome-next.jgi.doe.gov/info/Sbicolor_v3_1_1">phytozome-next.jgi.doe.gov/info/Sbicolor_v3_1_1</a>
<i>Sorghum bicolor</i> var <i>Rio</i>	v2.1	JGI-CSP	4558	<a href="https://phytozome-next.jgi.doe.gov/info/SbicolorRio_v2_1">phytozome-next.jgi.doe.gov/info/SbicolorRio_v2_1</a>
<i>Sphagnum angustifolium</i>	v1.1	Gene Atlas	53036	<a href="https://phytozome-next.jgi.doe.gov/info/Sfallax_v1_1">phytozome-next.jgi.doe.gov/info/Sfallax_v1_1</a>
<i>Setaria italica</i>	v2.2	Gene Atlas	4555	<a href="https://phytozome-next.jgi.doe.gov/info/Sitalica_v2_2">phytozome-next.jgi.doe.gov/info/Sitalica_v2_2</a>
<i>Setaria viridis</i>	v2.1	Gene Atlas	4556	<a href="https://phytozome-next.jgi.doe.gov/info/Sviridis_v2_1">phytozome-next.jgi.doe.gov/info/Sviridis_v2_1</a>

142

143 We sought to limit among-experiment measurement and environmental variation by using identical molecular  
144 methods to extract (RNA integrity number, RIN  $\geq 5$  and at least 1  $\mu$ g of total RNA) and sequence (Illumina  
145 stranded, paired-end 2x150 RNA-seq libraries) high-quality RNA. All samples were quality tested and  
146 sequenced at JGI. The resulting transcript abundance assays were highly correlated across biological replicates  
147 within conditions, tissues, and genotypes (**Supplemental Data 1**), which provides evidence that our gene  
148 expression measurements are highly accurate and robust.

149 We also demonstrated that the JGI Gene Atlas is updateable, with a new reference genome version and even  
150 with sequence data derived from other experiments and sequencing facilities. To accomplish this, we included  
151 *S. bicolor* 'Rio' (sweet sorghum,  $n_{samples} = 94$ ) (Cooper et al. 2019) from JGI's Community Science Program  
152 project and *Lupinus albus* (white lupin) cluster root tissue ( $n_{samples} = 72$ ) (Hufnagel et al. 2020) from a non-JGI  
153 project. A comprehensive list of all samples available so far is in **Supplemental Data 2** and  
154 <https://plantgenetlas.jgi.doe.gov>. Our custom pipeline to analyze expression levels of protein-coding genes is  
155 outlined in **Supplemental Fig. 2**.

156



157

158

159 **Figure 1 | The phylogenetic context and scope of Gene Atlas RNA-seq samples.** The 16 genomes are ordered by their  
160 phylogenetic position, visualized on the left as a cladogram without branch lengths that was constructed from 10 single-copy  
161 orthologs. Tips are labeled with genome names and thumbnail photos. Photo credit given on Phytozome.

162

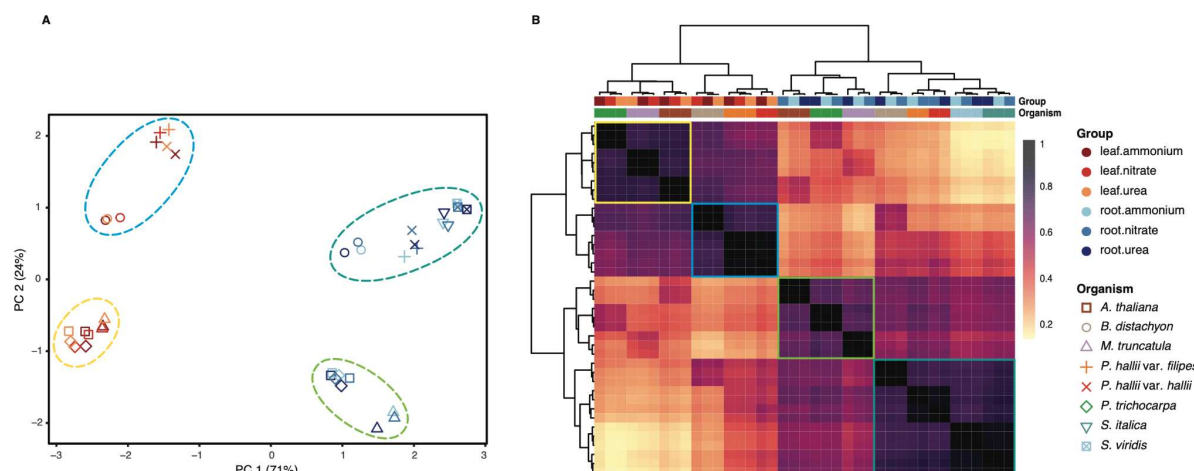
## 163 OVERVIEW OF THE TRANSCRIPTOMIC LANDSCAPE OF GENE ATLAS PLANTS

164 **Developing a baseline of evolutionarily conserved gene expression.** Across all 18 species, 47-87% (mean =  
165 73%) of annotated genes were transcriptionally active (FPKM  $> 1$ ). To test for conserved and divergent  
166 expression levels across the 18 species, we applied the traditional method of comparing single-copy orthologs  
167 across species. While powerful, restricting tests to orthologs based on gene sequences can be problematic  
168 across evolutionarily diverged lineages. For example, given the phylogenetic distance and nested whole-  
169 genome duplications among our sampled species, we were only able to find 2,066 one-to-one orthologous  
170 protein-coding genes (**Supplemental Data 3**) across just eight of the vascular plant genomes. Furthermore,  
171 such single-copy orthologs have evolutionarily conserved sequences and likely gene functions, permitting  
172 better homology-based functional descriptions (89.01% with good functional descriptions) than genome-wide  
173 averages (83.8%, Fisher's exact test odds = 1.607,  $P = 5.495e-12$ ). Nonetheless, we observed 227 (10.98%)  
174 genes with 1:1 orthologs and consistent expression among species, but weak functional descriptions  
175 (**Supplemental Data 4**). Given the expected paucity of multi-genome single-copy orthologs, we also addressed  
176 the challenge of finding genes with similar expression across species by analyzing pairwise single-copy

177 orthologs to a single reference genome, *A. thaliana*. Overall, we identified 6,018 unique *Arabidopsis* orthologs  
178 that showed conserved expression patterns across multiple species. Surprisingly, these genes include 660  
179 (11%) with little to no known functional description, making these genes rational targets for functional  
180 characterization studies (**Supplemental Data 5**). Identifying and improving the functional characterizations of  
181 such genes was one of the objectives of the Gene Atlas experiment. Genes with single-copy orthologs in *A.*  
182 *thaliana* and consistent expression were significantly enriched in transcription factors ( $n = 501$ , 8.3%; Fisher's  
183 exact test odds ratio = 1.507,  $P = 4.26e-13$ ), suggesting that potential regulators of different biological  
184 processes are strongly conserved across the plant species (Keightley and Hill 1990). These observed  
185 evolutionarily conserved expression patterns inform functional details that complement direct sequence data  
186 comparisons.

187 In contrast to these ortholog-constrained analyses, co-expression analyses are agnostic to orthology, which  
188 dramatically increases the number of genes that can be analyzed, providing a broader perspective on gene  
189 expression regulatory evolution. For example, multidimensional scaling and hierarchical clustering revealed that  
190 phylogenetically neighboring species have more similar expression profiles across tissues and nitrogen  
191 treatments than more distantly related species (Mantel  $R > 0.63$ ,  $P < 0.04$ ) (**Fig. 2**). However, the phylogenetic  
192 signal of co-expression was dwarfed by variation among tissues, where far more of the total co-expression  
193 clustering across nitrogen source treatments was driven by patterns among tissues than genetic distance  
194 among species (tissues correlated with the first canonical correspondence analysis axis, which explains 41.46%  
195 of the variation), suggesting that genes in closely related species exhibit similar transcriptional profiles across  
196 tissues and conditions likely owing to the accumulation of evolutionarily conserved regulatory elements.

197



198

199

200 **Figure 2 | Global patterns of gene expression across eight vascular plants.** Multidimensional scaling based on the  
201 expression of 2,066 single-copy orthologous genes in two tissues and three nitrogen treatment conditions show predominant  
202 clustering first by tissues and then by clade (mono-, dicots) (A). Hierarchical clustering based on Pearson correlation coefficients of  
203 log<sub>2</sub> transformed normalized expression data (B).

204

#### 205 **Patterns of tissue-specific gene expression across 18 species and >400M years of plant evolution.**

206 Tissue-specific expression complements global co-expression analyses by defining potential gene function  
207 associated with an organ or tissue. The major drawback of this approach results from morphological  
208 differences among species. For example, in *Chlamydomonas*, a single-celled organism, transcriptionally active  
209 genes in a given condition represent expressed genes in the organism as a whole, whereas multicellular  
210 organisms exhibit gene expression variation across different cell subtypes. Furthermore, the mosses sampled  
211 here lack root systems, flowers, seeds or easily sampled reproductive organs. Even the far more closely related  
212 flowering plants have functionally divergent homologous structures, such as root nodules, panicles, florets,  
213 sepals, and rhizomes. As such, analysis of tissue-specific expression must be somewhat phylogenetically  
214 constrained and condensed into large-scale functional tissue types (**Fig. 1**).

215 Our data suggest that large proportions of annotated genes ( $M = 44.7$ ;  $SD = 12.7$ ) are commonly  
216 expressed ( $FPKM > 1$ ) in multiple tissues (**Supplemental Data 6**), confirming that many genes serve multiple  
217 functions across tissues and environments. However, there was considerable among-tissue variation across

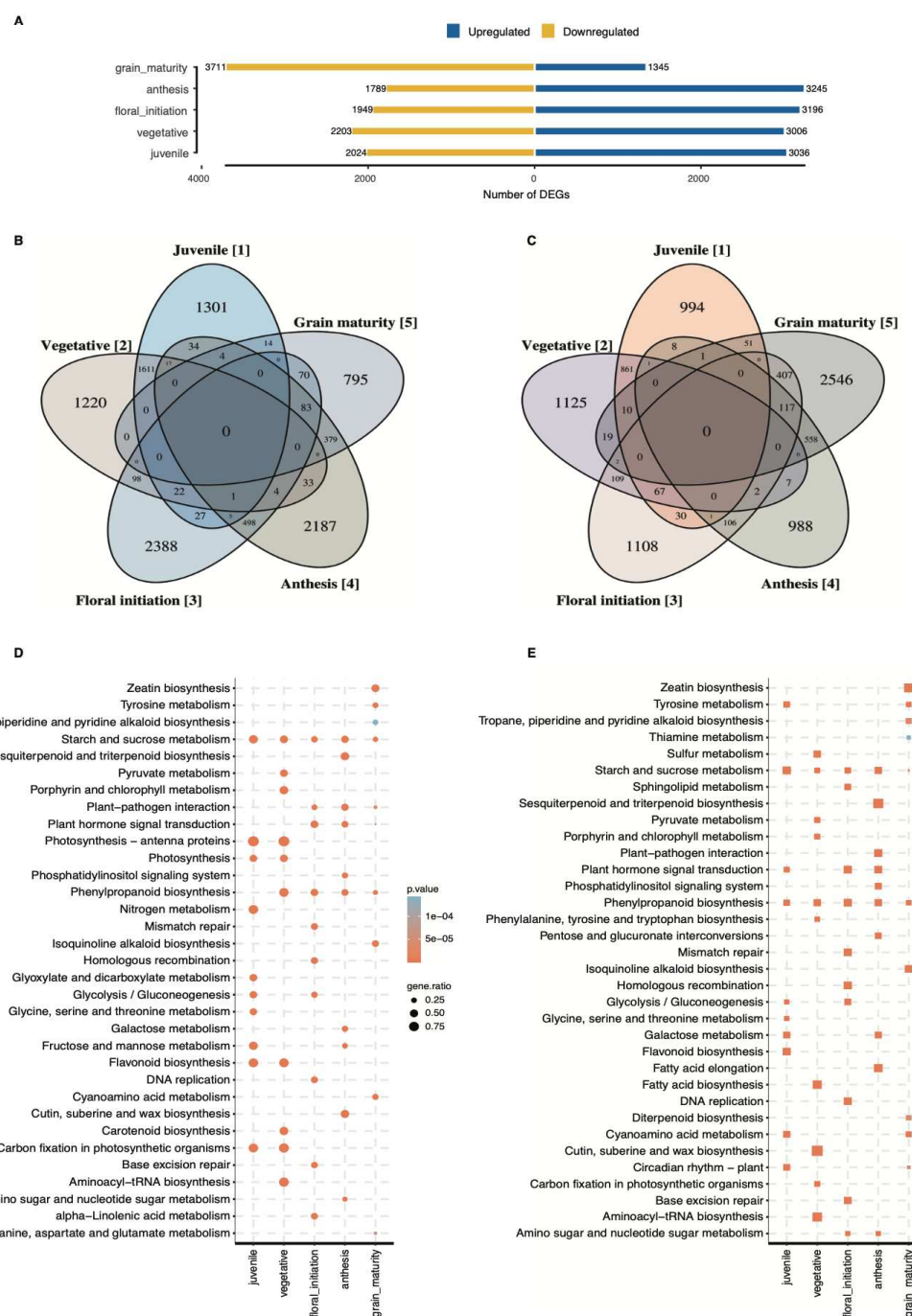
218 species (ANOVA  $F = 70.01$ ,  $df = 16$ ,  $P < 2e-16$ ) where gene expression is driven by variation among tissues or  
219 conditions (**Supplemental Data 6**). Such variably expressed genes may have evolved diverse functions  
220 depending on the regulatory environment across cell types.

221 Despite considerable across-tissue expression, we observed 220,218 (32.1%) of all genes with high expression  
222 specificity to a single tissue or condition. To identify genes exhibiting such strong tissue or condition specific  
223 expression, we used the Tau method (Yanai et al. 2005) which accounts for the number of unique sample types  
224 and produces consistently robust results with highest correlation between datasets of varying sizes  
225 (Kryuchkova-Mostacci and Robinson-Rechavi 2017). Using this method, we identified genes specific to (1)  
226 reproductive and root tissue in *S. italica*, (2) leaf, inflorescence, and whole floret in switchgrass, (3) leaf, leaf  
227 blade, dry seed, and imbibed seed in *S. bicolor*, and (4) stem and flower related gene sets in *Brachypodium*. Of  
228 all the standard plant tissues, stem and leaf had the fewest uniquely expressed genes (two-tailed unpaired  
229 Welch's t-test,  $P = 8.338e-06$ ) while roots followed by flower tissues were most unique (two-tailed unpaired  
230 Welch's t-test,  $P = 2.547e-10$ ). Groups of genes with greater expression proclivity towards spores, protonema  
231 and leaflet were recognized in *Physcomitrium*; drought and high temperature in *Sphagnum*; and towards seed,  
232 root tip, lateral root, and nodules in soybean (**Supplemental Data 7, 8**). These gene sets were largely  
233 overrepresented in GO biological processes known for each tissue or condition (**Supplemental Data 9**). Genes  
234 and their promoter regions with such marked expression specificity represent valuable tissue-specific reporters  
235 and targets for plant genetic engineering applications.

236

237 **Transcription modulation across developmental stages.** Developmental time-courses represent a  
238 particularly powerful experiment to understand gene function and the dynamics of transcript abundance. As an  
239 example of such a time course, we evaluated the regulation of gene expression in leaf tissue in five  
240 developmental stages of *Sorghum bicolor* (juvenile, vegetative, floral initiation, anthesis and grain maturity).  
241 Overall, we identified 13,992 unique DEGs ( $n$  total annotated genes= 34,211) across the five developmental  
242 stages (**Fig. 3A, 3B, 3C**). KEGG pathway enrichments of up-regulated differentially expressed genes were  
243 largely consistent with physiological expectations: photosynthesis, carbohydrate and N metabolism terms were  
244 overrepresented in juvenile/vegetative stages ( $P < 0.05$ , hypergeometric test), floral initiation/anthesis stages  
245 were enriched in reproductive organ development and hormone signal transduction, and grain maturity stage  
246 were enriched for amino acid metabolism and transport, and zeatin and tyrosine metabolism (**Fig. 3D, 3E**). We  
247 observed the enrichment pattern to be reversed among downregulated genes in different stages, e.g., plant-  
248 pathogen interaction and plant hormone signal transduction were suppressed in juvenile and vegetative stages  
249 whereas photosynthesis, carbohydrate and N metabolism related pathways were among those suppressed in  
250 late developmental stages (**Supplemental Fig. 3**). These overrepresented pathways among DEGs at each stage  
251 illustrate the key biological events over the growing season, e.g., as juveniles the *S. bicolor* are collecting  
252 energy to increase the biomass, and as they flower and mature, they express defense mechanisms, and finally,  
253 with grain maturity, they reduce photosynthesis and slow down nutrient acquisition. The *S. bicolor* dataset  
254 provides an example of high-resolution characterization of gene expression changes and insight into the  
255 molecular responses of the plant across developmental stages represented by the Gene Atlas dataset.

256



257

258 **Figure 3 | Differentially expressed gene comparison across five developmental stages in *Sorghum bicolor*.** Numbers of  
259 differentially expressed genes across developmental stages (A). Venn diagrams of up-regulated (B) and down-regulated genes that  
260 are unique and shared between developmental stages (C). Top 10 KEGG metabolic pathway enrichments ( $P < .05$ , hypergeometric  
261 test) of up-regulated differentially expressed genes in each of the five developmental stages (D) and upregulated genes unique to  
262 each stage (E). 'gene.ratio' represents the ratio of number of DEGs over the number of genes annotated specific to the pathway.

263

264

265

266

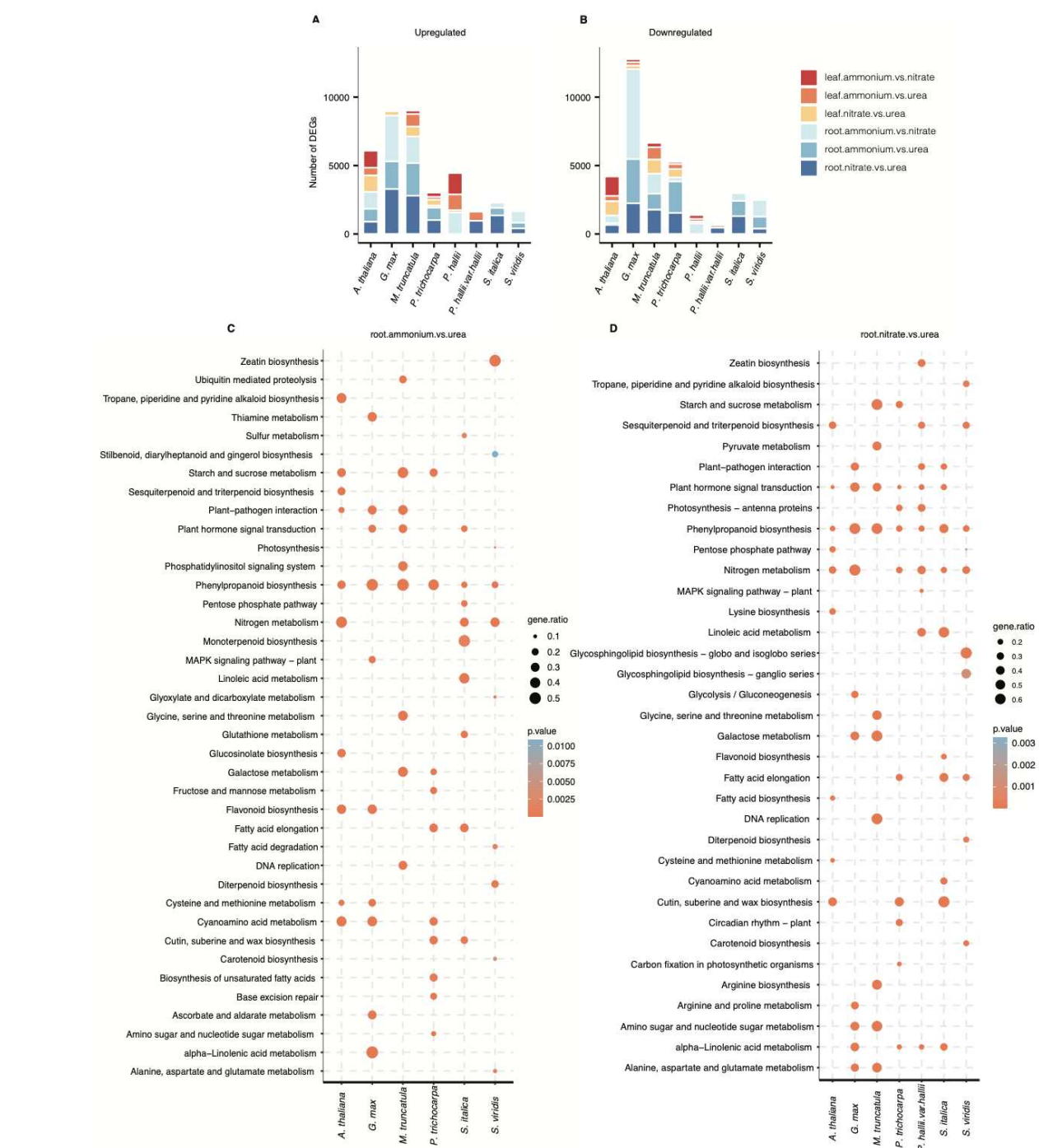
267

268

269 **Transcriptional responses to different N sources.** Tissue-specific gene expression regulatory responses to  
270 environmental cues are often evolutionarily conserved. These conserved responses offer a framework to test  
271 hypotheses about gene function as it relates to environmental sensitivity. A particularly powerful experiment  
272 adjusts the amount and type of necessary resource available. Drought, light and nutrient availability  
273 manipulations have provided strong evidence for gene function across the diversity of plants (Faye et al. 2022);  
274 (Zhang et al. 2021); (Huang, Zhao, and Chory 2019); (Swift et al. 2020); (Y. Li et al. 2022). In addition to providing  
275 evidence for the function of specific candidate genes' responses to environmental stimuli, highly controlled  
276 manipulations, like our nitrogen source experiments, offer a framework to compare the relative roles of gene  
277 families and molecular pathways.

278 To understand gene expression underpinnings of N metabolism, we contrasted transcript abundance in  
279 aboveground and root tissues of each Gene Atlas species (where available, see **Fig. 1**) grown on N from three  
280 sources: urea, ammonium ( $\text{NH}_4^+$ ), and nitrate ( $\text{NO}_3^-$ ) (**Supplemental Data 10**). Since our experiments had similar  
281 statistical power and biological replicates among species and conditions, the total number of DEGs is a strong  
282 indicator of the transcriptional effects of different N sources. The most striking patterns were those related to  
283 tissue-specific gene expression variation within genotypes (**Fig. 4A, 4B**). For example, the root transcriptome  
284 was more responsive than aboveground tissues in all eudicot genotypes (Mann-Whitney U-test,  $P = 5e-04$ )  
285 except *Arabidopsis* (two-tailed unpaired Welch's t-test,  $P = 0.4526$ ). We observed consistent enrichments of N  
286 metabolism pathway genes among differentially expressed genes between treatments across many species,  
287 which demonstrates that this experiment elicits molecular responses of genes with homologs in genetic model  
288 species.

289 Despite the power of discovering enriched groups of genes with similar and expected functional annotations, a  
290 major goal of the Gene Atlas is to provide a framework to discover novel gene functions and interactions. As  
291 such, we were excited to find starch and sucrose metabolism, and phenylpropanoid biosynthesis pathways  
292 overrepresented in upregulated DEGs. Indeed, many of the DEGs we identified in pairwise comparisons  
293 between N-sources are not directly involved in N metabolism. For example, genes associated with plant-  
294 pathogen interaction, plant hormone signal transduction, and carbohydrate metabolism were abundant (**Fig.**  
295 **4C, 4D, Supplemental Fig. 4**). Similar observations were reported previously in *Sorghum* genotypes with  
296 varying N-stress tolerance subjected to N-limiting conditions (Gelli et al. 2014). Notably, nitrogen and amino  
297 acid metabolism-related pathways were overrepresented mainly in DEGs in nitrate vs. urea comparison. Such  
298 comparisons highlight differences in plant's response to  $\text{NO}_3^-$  as a sole N source compared to  $\text{NH}_4^+$  at the  
299 metabolic level.



300

301 **Figure 4 | Transcriptional response of Gene Atlas plants towards  $\text{NH}_4^+$  and  $\text{NO}_3^-$  compared to urea as the sole nitrogen**  
302 **source in root and leaf tissues.** Numbers of genes differentially upregulated (A) and numbers of genes differentially  
303 downregulated in response to changing nitrogen regime (B). Top 10 KEGG metabolic pathway enrichments ( $P < .05$ ,  
304 hypergeometric test) in up-regulated differentially expressed genes in roots from Gene Atlas plants in ammonia vs. urea (C)  
305 and nitrate vs. urea treatment comparisons (D). 'gene.ratio' represents the ratio of number of DEGs over the number of genes  
306 annotated specific to the pathway.

307

308

309

### 310 INFERRING GENE FUNCTION FROM PATTERNS OF GENE EXPRESSION

311 **Variation in co-expression network topologies.** Genes with similar expression patterns across diverse  
312 environmental conditions and tissues tend to serve similar biological functions across distantly related species  
313 and can be detected by co-expression clustering algorithms. For example, clusters of genes associated with a  
314 specific tissue or condition may be crucial for plant development or response to environmental cues. These  
315 strongly conserved tissue- and treatment-specific expression patterns facilitate biological gene function  
316 extrapolating from expression studies in one organism to close phylogenetic neighbors. To identify modules  
317 with such coherent expression patterns, we constructed 30 weighted gene co-expression networks (Langfelder  
318 and Horvath 2008) and 148 highly significant (min KME = 0.7, cut height = 0.25) co-expression modules within  
319 species and across different sets of tissues and conditions. Of these, 21 modules were significantly correlated  
320 with stress treatments (i.e., heat, cold, drought, salt, and wound stresses), 10 with N treatments, and 33 with  
321 other experimental conditions (**Supplemental Data 11**). Tissue-specific modules were also very common, e.g.,  
322 root tissue-specific modules (n = 11), contained genes with GO terms enriched in responses to stimulus,  
323 oxidation-reduction process (Manzano et al. 2014; Passaia et al. 2014) and hydrogen peroxide metabolism (Ma  
324 et al. 2014) that are relevant to root functions (Bruex et al. 2012; Kogawara et al. 2014; W. Li, Lan, and 3.948  
325 2015; Loreti et al. 2005). Leaf specific modules (n = 11) were enriched for phototropism, thylakoid membrane  
326 organization, pigment biosynthetic process, phototropism, and carbon fixation (**Supplemental Data 12**),  
327 suggesting that genes within the same module are associated with the same or interconnected biological  
328 functions.

329  
330 **Inferring transcription factor functions from co-expressed genes.** Genes showing highest connectivity with  
331 neighboring genes within a module, referred to as hub genes, are likely involved in preserving multi-gene  
332 regulatory variation and thus network integrity, potentially as trans-regulatory elements like transcription factors.  
333 We determined the top 10 most highly connected hub genes within each module. Across all the co-expression  
334 networks 87 hub genes belonged to transcription factor (TF) families (via PlantTFDB; (Jin et al. 2017))  
335 (**Supplemental Data 13**), a slight but not significant enrichment of TFs relative to the genomic background (%  
336 hub TFs = 6.21%, background TFs = 5.23%, Fisher's exact test odds ratio = 0.834,  $P = 0.104$ ). TFs with many  
337 connections are presumed to be most influential in regulating the expression of modular genes in co-expression  
338 networks (Mukhtar et al. 2011). Under this premise, we further explored the overrepresented TF families among  
339 the hub genes. Most represented TF families in N treatment modules were MYB, WRKY, and NAC. Similar  
340 observations were made by Canales et al. (Canales et al. 2014) from *Arabidopsis* root transcriptomic data  
341 generated under contrasting N conditions. As shown in previous studies (Ghazalpour et al. 2006; Horvath et al.  
342 2006; Liu, He, and Deng 2021; Miller, Oldham, and Geschwind 2008; Torkamani et al. 2010; Voineagu et al.  
343 2011), hub genes play key roles in orchestrating module behavior and provide a specific focus for investigations  
344 into trait or condition related modules.

345  
346 **Expression derived function descriptions (EDFD).** To evaluate how well the predicted gene function  
347 descriptions of Gene Atlas plants illustrate validated gene functions, we categorized currently assigned  
348 functional descriptions available at Phytozome as genes with good (GGF) and poor (GPF) function descriptions  
349 using an augmented dictionary lookup approach that incorporates weighting for negative, positive, and  
350 adversative keywords. Overall, 16% to 56% of the functional descriptions are GPF across the plants, with a  
351 large percentage of such genes not having a known function (**Supplemental Fig. 1**) (Gollery et al. 2006; Rhee  
352 and Mutwil 2014). We then assigned EDFD to the two subsets using results from tissue and condition specific  
353 expression groups, DEGs unique to a single contrast and co-expression network analysis along with ortholog  
354 function descriptions derived from nearest phylogenetic neighbors (see Methods).

355  
356 Using this method, we added additional biological information to an average of 40.6% ( $SD = 12.6$ ) of genes  
357 (excluding orthology based function descriptions) in these plant genomes (**Table 2; Supplemental Data 14**).  
358 For example, in the case of *S. bicolor*, 5,357 (15.65% of the total) genes lacked sequence homology-based  
359 function descriptions, 24,406 had good functional descriptions while overall 9,723 had poor descriptions. Gene  
360 Atlas expression-based functional descriptions were assigned to a total of 20,259 genes, of which 14,891  
361 (43.63% of total annotated genes) had good functional descriptions and 5,368 (15.73%) had poor descriptions.  
362 To verify the reliability of the assigned functional associations, GO enrichment analysis of genes assigned with  
363 descriptions based on leaf and root samples was performed. We observed significant enrichment for  
364 photosynthesis, chloroplast organization, chlorophyll biosynthetic process and plastid translation ( $P < .05$ ,  
365 Fisher's exact test) in leaf related EDFDs; and cell wall loosening (Somssich, Khan, and Persson 2016), water  
366 transport and xyloglucan biosynthetic process (Peña et al. 2012) ( $P < .05$ , Fisher's exact test) in root related

367 EDFDs. Similar analysis in *Brachypodium* genes with assigned descriptions based on abiotic stress  
368 experiments (i.e., cold, heat, drought, and salt stress) showed significant enrichment for regulation of cellular  
369 response to alkaline pH, response to cold, heat, and positive regulation of response to oxidative stress ( $P < .05$ ,  
370 Fisher's exact test). Likewise, among genes annotated based on flower samples, specification of floral organ  
371 identity, fruit wall development and sporopollenin biosynthetic process were among the top enriched GO terms  
372 ( $P < .05$ , Fisher's exact test). These results indicate that the assigned functional descriptions show strong  
373 biological role predictability and the approach here aids in expanding our current understanding of plant gene  
374 functions.

375

376 **Table 2 | Summary of assigned expression derived function descriptions (EDFD) to Gene Atlas.** Number of annotated  
377 genes and the percentage of genes with good function descriptions (GGF), poor function descriptions (GPF) categorized using an  
378 augmented dictionary lookup approach that incorporates weighting for negative, positive, and adversative keywords and  
379 percentage of genes assigned with expression derived function descriptions.

Genome	n.genes	% GGF	% assigned (GGF)	% GPF	% assigned (GPF)	n.assigned	% assigned (total)
<i>A. thaliana</i>	27,416	83.86	32.43	16.14	5.573	10,418	38.00
<i>B. distachyon</i>	34,310	72.56	34.17	27.44	13.19	16,247	47.35
<i>C. reinhardtii</i>	17,741	43.08	12.6	56.92	15.98	5,070	28.58
<i>E. grandis</i>	36,349	79.74	28.63	20.26	3.997	11,858	32.62
<i>G. max</i>	52,872	80.37	47.25	19.63	11.33	30,971	58.58
<i>K. fedtschenkoi</i>	30,964	82.01	39.56	17.99	7.644	14,615	47.20
<i>M. truncatula</i>	50,894	67.94	23.66	32.06	5.285	14,731	28.94
<i>P. hallii</i>	33,805	72.65	34.97	27.35	8.656	14,746	43.62
<i>P. halliiHAL</i>	33,263	73.36	31.16	26.64	7.946	13,007	39.10
<i>P. patens</i>	32,926	55.44	19.35	44.56	14.06	11,003	33.42
<i>P. trichocarpa</i>	34,699	82.31	39.57	17.69	7.997	16,507	47.57
<i>P. virgatum</i>	80,278	69.2	39.73	30.8	14.15	43,251	53.88
<i>S. bicolor</i>	34,129	71.51	43.63	28.49	15.73	20,259	59.36
<i>S. bicolorRio</i>	35,490	69.16	15.04	30.84	4.765	7,029	19.81
<i>S. fallax</i>	25,100	78.31	32.36	21.69	9.183	10,427	41.54
<i>S. italicica</i>	34,584	77	39.37	23	10.78	17,344	50.15
<i>S. viridis</i>	38,334	70.43	35.99	29.57	12.74	18,680	48.73
<i>L. albus</i>	38,258	78.17	11.01	21.83	2.415	5,138	13.43

380

381 To help investigators target important genes for additional functional studies, we ranked the biological  
382 relevance of genes using a scoring methodology based on expression patterns of genes identified using  
383 tissue/condition specificity, differential expression, co-expression, hub status in a co-expression module and  
384 consensus expression across species. Gene orthologs with similar expression profiles in two or more species  
385 were given additional scores derived from the phylogenetic distance, i.e., larger the divergence time higher the  
386 score (see Methods). We identified a total of 656 top ranked genes across Gene Atlas plants (604 have  
387 orthologs in  $\geq 5$  plants; 40 of which have orthologs in  $\geq 10$  of evaluated plants) that have poor functional  
388 information but with the potential to improve our understanding of plant biology and form a list of prioritized  
389 targets for future experimental investigations (**Table 3; Supplemental Data 15**).

390

391

392

393

394 **Table 3 | Prioritized top ranked genes with poor functional descriptions for future experimental investigations.** Genes  
 395 were given scores based on expression patterns identified from i) unique differential expression in a single contrast, ii)  
 396 tissue/condition specific expression and iii) biologically relevant co-expression modules (each given a score of 2) while hub  
 397 genes in a co-expression module were given a score of 4. Gene orthologs with similar expression profiles were given  
 398 additional scores derived from the phylogenetic distance. Total score was calculated as the aggregate of individual scores.  
 399 Top ranked genes (two per species) are represented here.  
 400

Organism	Gene ID	Score					Arabidopsis orthologs	
		Differential expression	Condition specific expression	Co-expression	Hub gene	Consensus expression		
<i>A. thaliana</i>	AT2G20080	2	2	2	0	21.91	27.91	AT2G20080
	AT4G28840	0	2	2	0	21.91	25.91	AT4G28840
<i>B. distachyon</i>	Bradi1g38210	0	2	2	0	10.7	14.7	AT2G42760
	Bradi2g23445	0	0	2	0	11.69	13.69	AT5G02090; AT2G37750
<i>C. reinhardtii</i>	Cre02.g078550	0	2	2	4	0	8	
	Cre02.g092700	0	2	2	4	0	8	
<i>E. grandis</i>	Eucgr.B00604	0	2	2	0	16.57	20.57	AT5G08050
	Eucgr.F01122	0	2	2	0	17.12	21.12	
<i>G. max</i>	Glyma.13G227500	0	0	2	0	20.28	44.56	AT1G33055
	Glyma.16G013600	0	0	2	0	20.84	45.68	AT3G14280
<i>K. fedtschenkoi</i>	Kaladp0065s0016	0	0	2	0	19.79	21.79	AT4G28840; AT2G20080
	Kaladp0965s0006	2	0	2	0	26.23	30.23	AT2G30230; AT1G06980
<i>M. truncatula</i>	Medtr2g079300	2	2	2	0	18.11	24.11	
	Medtr3g031140	0	2	2	0	27.28	31.28	AT2G30230; AT1G06980
<i>P. hallii var. filipes</i>	Pahal.3G090000	2	2	2	0	13.2	19.2	AT5G02160
	Pahal.7G305700	2	2	2	0	12.05	18.05	AT4G21445
<i>P. hallii var. hallii</i>	PhHAL.3G160400	0	0	2	0	14.55	16.55	
	PhHAL.5G229300	2	2	2	0	11.532	17.532	AT5G62770; AT3G27880; AT1G23710; AT1G70420
<i>P. patens</i>	Pp3c11_15500	2	2	2	4	0	10	
	Pp3c13_2427	0	2	2	4	0	8	
<i>P. trichocarpa</i>	Potri.018G084100	2	2	2	0	19.79	25.79	AT4G28840; AT2G20080
	Potri.003G193400	2	0	2	0	20.89	24.89	
<i>P. virgatum</i>	Pavir.5NG404000	0	0	2	0	13.64	15.64	
	Pavir.2NG640501	0	2	2	0	9.72	13.72	AT5G13720
<i>S. bicolor</i>	Sobic.009G229000	0	0	2	4	13.35	19.35	AT4G28840; AT2G20080
	Sobic.001G118400	2	2	2	0	10.44	16.44	AT1G73885
<i>S. bicolor</i> Rio	SbRio.08G154700	0	2	2	0	12.31	16.31	AT5G08050
	SbRio.10G134000	0	2	2	0	12.05	16.05	AT4G01150
<i>S. angustifolium</i>	Sphfalx02G142200	2	2	2	4	0	10	
	Sphfalx11G077900	2	2	0	0	4.5	8.5	AT3G03341
<i>S. italicica</i>	Seita.9G407600	2	0	2	0	12.7053	16.7053	AT1G63410; AT3G14260
	Seita.9G436900	0	2	2	0	12.5741	16.5741	AT2G30230; AT1G06980
<i>S. viridis</i>	Sevir.1G151100	2	0	2	0	13.2732	17.2732	AT1G12320; AT1G62840; AT3G60780; AT2G45360
	Sevir.5G247600	0	0	2	0	13.2732	15.2732	AT5G62770; AT3G27880; AT1G23710; AT1G70420

## 402 DATA ACCESS

403 JGI Plant Gene Atlas data are currently hosted at two portals: i) JGI Plant Gene Atlas  
404 (<https://plantgeneatlas.jgi.doe.gov>), a dedicated portal provides bulk access to the data and user-specified  
405 queries of a single gene to multiple gene sets, lets users access differentially expressed genes, visualize gene  
406 ontology and pathway enrichments and track orthologs across the Gene Atlas plants; and ii) JGI's plant portal,  
407 Phytozome ([phytozome.jgi.doe.gov](https://phytozome.jgi.doe.gov)). Currently, Phytozome provides efficient tabular and graphical  
408 representation of co-expressed genes, pathway details, peptide, CDS and transcript sequence, protein  
409 homologs, plant family information and additionally genome browser view of gene models.

410

## 411 CONCLUSIONS

412 Here we analyzed the transcriptional landscape of 18 plants from 2,090 RNA-seq datasets. To the best of our  
413 knowledge, it is the largest compendium of plant transcriptome data generated following standardized  
414 protocols across diverse plant species. These datasets enable JGI's efforts to improve genome annotations  
415 especially related to conserved biological processes across the diversity of plants. Comparing orthologs among  
416 common gene sets between species allowed us to pinpoint and rank biologically relevant and evolutionarily  
417 conserved genes, demonstrating the potential of cross-species analysis from the transcriptome resource  
418 generated in this study. Furthermore, our results documented plant responses to varying N resources at the  
419 organ level and expression variation among developmental stages. These and other analyses highlight shared  
420 and varied gene expression regulatory evolution across plants.

421 The Gene Atlas datasets, along with the additional expression derived functional annotations, are valuable  
422 resources to the plant research community and provide targets, unknown or poorly described TFs, hub genes,  
423 and conserved genes, for functional studies that directly improve gene functional descriptions. We  
424 acknowledge that these functional associations are not definitive evidence of their functions, but we anticipate  
425 that they will be useful in directing future functional characterization experiments. We will continue to expand  
426 the Gene Atlas through standardized procedures to increase the specificity of these function descriptions. We  
427 strongly believe that results from this study and additional custom analyses on this resource will aid researchers  
428 in better understanding of roles of genes in their own experiments and get a better handle on biological  
429 processes at the system level.

430

## 431 METHODS

### 432 Plant growth and treatment conditions

433 **Glycine max and Medicago truncatula.** Plant seeds (*G. max* cv. Williams 82) were surface-sterilized, transferred to pots  
434 containing 3:1 vermiculite perlite. 2/3 seedlings were planted in each pot and grown until plants were 4 weeks in a growth  
435 chamber under 16 h-light/8 h-dark conditions, 26–23°C temperature maintained at 250  $\mu\text{mol m}^{-2}\text{s}^{-1}$ . Plants for nitrogen  
436 experiment were watered with nutrient solution containing either 10 mM  $\text{KNO}_3$  ( $\text{NO}_3^-$  plants) or 10 mM  $(\text{NH}_4)_3\text{PO}_4$  ( $\text{NH}_4^+$  plants)  
437 or 10 mM urea (urea plants). We selected urea as a control condition for the counter ions, potassium, and phosphate, as the  
438 best compromise. The nutrient solutions were renewed every 3 days. After 4 weeks, different tissues (leaf, stem, root, shoot,  
439 shoot tip, root tip, lateral roots, etc) for N regimes and standard conditions were harvested. Plants under symbiotic conditions  
440 were watered with nutrient solution containing 0.5 mM  $\text{NH}_4\text{NO}_3$  every other week. Subsequently, root nodules, roots, and  
441 trifoliate leaves under symbiotic conditions were collected and tissues from flower open and un-open were harvested from  
442 field grown plants.

443 **Arabidopsis thaliana.** Seeds were cold-stratified in water for 3 days and subsequently seeds were sown into 9  $\text{cm}^2$  plastic  
444 pots (T.O. Plastics, Clearwater, FL, USA) filled with 2 parts Promix Biofungicide (Premier Tech, Rivière-du-Loup, QC, Canada)  
445 to 1 part Profile Field and Fairway (Profile, Buffalo Grove, IL, USA). Pots were placed in a growth chamber (22°C days/20°C  
446 nights, 14 h light at a photosynthetic photon flux density of 350  $\mu\text{mol m}^{-2}\text{s}^{-1}$ ), then thinned to 1 plant per pot containing  
447 Sunshine MVP potting mix (SunGro Horticulture) and transferred into a greenhouse at the University of Texas at Austin when  
448 rosettes had achieved 7–8 leaves. Plants supplemented with differing nitrogen source regimes (see *Glycine max*) were  
449 harvested after 30 days.

450 **Brachypodium distachyon.** Seeds (*B. distachyon* Bd21) were grown in Metro mix 360 soil in a growth chamber, under 12 h  
451 day and 12 h night conditions, maintained at 24°C/18°C, ~50% relative humidity; 150  $\mu\text{mol m}^{-2}\text{s}^{-1}$ . Plants were watered once  
452 a day or every two days depending on the size of plants and soil conditions and fertilized twice a week (Tuesday and Friday)  
453 using Jack's 15-16-17 at a concentration of 100 ppm. For the nitrogen source study, plants grown for 30 days under differing  
454 nitrogen source regimes (see *Glycine max*) were harvested.

455 For cold treatment experiment, Bd21 seeds were sown in soil without stratification. The germinated seeds were grown in a  
456 growth chamber under short day conditions (26°C 10 h light, 18°C 14 h dark) for 4 weeks and then moved to a cold room

457 (4°C 10 h light, 4°C 14 h dark) for cold treatment. Whole shoots were harvested at different treatment time points and stored  
458 at -80°C for RNA extraction.

459 ***Chlamydomonas reinhardtii***. *C. reinhardtii* strain CC-1690 (also known as 21gr) was cultured at 24°C (agitated at 180 rpm at  
460 a photon flux density of 90  $\mu\text{mol m}^{-2}\text{s}^{-1}$  provided by cool white fluorescent bulbs at 4100 K and warm white fluorescent bulbs  
461 at 3000 K used in the ratio of 2:1) in tris acetate-phosphate (TAP) medium (Boyle et al. 2012). For growth in differing nitrogen  
462 sources, TAP medium was supplemented with  $(\text{NH}_4)_3\text{PO}_4$  or  $\text{KNO}_3$ , or urea (see *Glycine max*). Cultures of strain CC-1690 were  
463 inoculated to  $1 \times 10^5$  cells  $\text{ml}^{-1}$  and collected for RNA at  $1 \times 10^6$  cells  $\text{ml}^{-1}$ , when the growth rates of all cultures were identical.  
464 For assessing the impact of cell density, cultures were inoculated at  $1 \times 10^4$  cells  $\text{ml}^{-1}$  in replete medium and sampled at  $5 \times$   
465  $10^5$  cells  $\text{ml}^{-1}$  and at each doubling thereafter until the culture reached a final density of  $8 \times 10^6$  cells  $\text{ml}^{-1}$ .

466 ***Eucalyptus grandis***. *E. grandis* samples were derived from tissues collected from clonal ramets of the genotype BRASUZ1  
467 that was used to generate the *E. grandis* reference genome. Tissue samples were collected from three trees ca. 5 years old,  
468 and an adult tree ca. 8 years old at the time of sample collection, planted in experimental fields at Embrapa Genetic  
469 Resources and Biotechnology in Brasilia, Brazil (15.73 South, 47.90 West). RNA samples were prepared from adult leaves  
470 (completely developed), juvenile leaves (tender, thinner, not waxed), fruit buds, and developing cambium (from inside the tree  
471 bark). Plant material was collected from the field, immediately frozen in liquid nitrogen, and stored at -80°C until RNA  
472 extraction that followed an optimized CTAB-lithium chloride-based protocol (Inglis et al. 2018).

473 ***Kalanchoë fedtschenkoi***. Four-week-old *K. fedtschenkoi* plants (accession ORNL M2) were grown under a  $250 \text{ mmol m}^{-2} \text{s}^{-1}$   
474 white light with a 12 h light (25°C)/12 h dark (18°C) cycle and were used as starting plant material for eight different  
475 experiments (i.e., circadian, metabolite, temperature, drought, light intensity, light quality, nitrogen utilization, and standard  
476 tissue). The experiments were conducted under day/night temperature regime of 25°C/18°C except the temperature  
477 experiment. For the circadian experiment, two sets of plants were grown under a 12 h light/12 h dark cycle and continuous  
478 lighting ( $250 \text{ mmol m}^{-2} \text{s}^{-1}$  white light), respectively, for seven days and then mature leaf samples (i.e., leaves 5-7 counting  
479 from the top of the plants) were collected every two hours over a 48 h period. For the metabolite experiment, plants were  
480 grown under an aerobic condition to prevent dark  $\text{CO}_2$  fixation and malate accumulation. This was accomplished by putting  
481 the plants in a sealed chamber with a closed air loop, through which air was continuously circulated.  $\text{CO}_2$  was subsequently  
482 continuously scrubbed from the air using a hydrated soda lime filter (LI-COR Biosciences, Lincoln NE) included in the loop.  
483  $\text{CO}_2$  levels were monitored and maintained at an average of 3 ppm over the 12 h overnight aerobic treatment. Plants were  
484 removed from the aerobic condition just prior to the start of the daylight photoperiod. Mature leaves were harvested at 2 h  
485 intervals over the succeeding 24 h period (12 h light/12 h dark). For the temperature treatment, plants were grown under three  
486 different temperatures (8°C, 25°C and 37°C), respectively, for seven days. For drought treatments, plants were grown under  
487 three soil moisture conditions ( $40\% \pm 3\%$  [control],  $20\% \pm 3\%$  [moderate drought] and  $2\% \pm 3\%$  [severe drought]),  
488 respectively, for 19 days. For the light intensity experiment, plants were grown under light intensity of 0 (darkness), 150 (low  
489 light) and 1000 (high light)  $\text{mmol m}^{-2} \text{s}^{-1}$  for 48 h. For the light quality experiment, plants were grown under blue light (270  
490  $\text{mmol m}^{-2} \text{s}^{-1}$ ), red light (280  $\text{mmol m}^{-2} \text{s}^{-1}$ ), far-red light (280  $\text{mmol m}^{-2} \text{s}^{-1}$ ) and constant darkness for 48 h. For the nitrogen  
491 utilization experiment, plants were treated with potassium sulfate (10 mM), ammonium sulfate (10 mM) and urea (5 mM),  
492 respectively, for four weeks. Immediately after the temperature, drought, light intensity, light quality and nitrogen utilization  
493 experiments, mature leaves were collected at two time points of dawn (2 h before the start of light period) and dusk (2 h  
494 before the start of dark period). For the nitrogen utilization experiment, root samples were also collected at dawn and dusk,  
495 respectively. For the standard tissue experiment, plants were grown in the greenhouse under a 12 h light/12 h dark cycle at  
496 Oak Ridge National Laboratory (Oak Ridge, TN) and five different tissue types (young leaf, young stem, mature stem, root,  
497 and flower) were collected at 10 am in the greenhouse.

498 ***Lupinus albus***. RNA-seq data from cluster root samples were obtained from (Hufnagel et al. 2020).

499 ***Panicum virgatum***. Vegetatively propagated Alamo AP13 plants were grown in pre-autoclaved MetroMix 300 substrate  
500 (Sungro® Horticulture, <http://www.sungro.com/>) and grown in a walk-in growth chamber at 30/26°C day/night temperature  
501 with a 16 h photoperiod ( $250 \mu\text{m}^{-2} \text{sec}^{-1}$ ) for four months. Tissues were harvested at six developmental stages, including leaf  
502 development (VLD: V2), stem elongation (STE: E2 and E4), and reproductive phases (REP: R2, S2, and S6) (Moore et al.  
503 1991).

504 For *P. virgatum* photoperiod experiment, four switchgrass genotypes, AP13, WBC, AP13, and VS16 plants were vegetatively  
505 propagated and grown in one-gallon pots with a 6:1:1 mixture of Promix:Turface:Profile soil at a growth chamber at the  
506 University of Texas at Austin. After one-week maintenance with a 30/25°C day/night temperature and 14L/10D photoperiod,  
507 plants from each genotype were divided into two groups and received LD (16L/8D) or SD (8L/16D) treatment in separate  
508 growth chambers. Fully emerged young leaves were simultaneously harvested from three individuals as three biological  
509 replicates after three-week LD and SD treatments. We collected two leaf tissues (2cm leaf tips and 2 cm leaf base) at two  
510 zeitgeber times (ZT1 and ZT17). All samples were immediately flash frozen in liquid nitrogen and stored at -80 °C for DNA and  
511 RNA extraction.

512 ***Panicum hallii***. The *P. hallii* FIL2 (var. *filipes*; Corpus Christi, TX; 27.65° N, 97.40° W) and *P. hallii* HAL2 (var. *hallii*; Austin, TX;  
513 30.19° N, 97.87° W) were grown in 3.78 L pots at the University of TX Brackenridge Field Laboratory (Austin, Texas) in the  
514 greenhouse with mean daytime air temperature of 30°C and relative humidity of 65%. Plants supplemented with differing  
515 nitrogen source regimes (see *Glycine max*) were harvested after 30 days.

516 For *P. hallii* panicle samples, genotypes, HAL2 and FIL2, were grown in a growth chamber at University of Texas at Austin  
517 with 26°C day/22 °C night temperature and 12 h photoperiod. Plants were grown in 3.5 inches square pots with a 6:1:1  
518 mixture of Promix:Turface:Profile soil. Young panicle tissues were collected under a dissection microscope and the

519 developmental stages were determined according to the lengths (0.1-0.2 cm for D1 stage, 0.5-1 cm for D2 stage, 4.5-5.5 cm  
520 for D3 stage, and 9-11 cm for D4 stage). Tissues for D1 and D2 stages were taken from at least fifty plants and pooled for  
521 each biological replicate. Tissues for D3 and D4 stages were taken from at least fifteen plants and pooled for each biological  
522 replicate. All samples were harvested at 17:00-18:00 of the day and immediately flash frozen in liquid nitrogen. Three  
523 biological replicates for each stage were stored at -80°C for DNA and RNA extraction.

524 ***Physcomitrium patens***. The protonemata cultures were systematically entrained by two successive weeks of culture prior to  
525 treatment to obtain a homogeneous culture as described in Perroud et al. (Perroud et al. 2018). In brief, BCD (Cove et al.  
526 2009) or Knop medium (Reski and Abel 1985) were used to culture the moss. Solid medium (medium with 1% [w/v] agar)  
527 protonemal cultures were grown atop a cellophane film to allow tissue transfer for specific treatments (e.g., with hormones),  
528 and for ease of harvesting. Plates and flasks were cultivated at 22°C with a 16 h-light/8 h-dark regime under 60-80  $\mu\text{mol}$   
529  $\text{m}^{-2}\text{s}^{-1}$  white light (long-day conditions). All harvests were performed in the middle of the light photoperiod (+8 h of light in  
530 long day conditions) (Perroud et al. 2018; Fernandez-Pozo et al. 2020).

531 ***Populus trichocarpa***. *Populus trichocarpa* (Nisqually-1) cuttings were potted in 4" X 4" X 5" containers containing 1:1 mix of  
532 peat and perlite. Plants were grown under 16 h-light/8 h-dark conditions, maintained at 20-23°C and an average of 235  $\mu\text{mol}$   
533  $\text{m}^{-2}\text{s}^{-1}$  to generate tissue for (1) standard tissues and (2) nitrogen source study. Plants for standard tissue experiment were  
534 watered with McCown's woody plant nutrient solution and plants for nitrogen experiment were supplemented with either  
535 10mM  $\text{KNO}_3$  ( $\text{NO}_3^-$  plants) or 10mM  $(\text{NH}_4)_3\text{PO}_4$  ( $\text{NH}_4^+$  plants) or 10 mM urea (urea plants). Once plants reached leaf  
536 plastochron index 15 (LPI-15), leaf, stem, root, and bud tissues were harvested and immediately flash frozen in liquid nitrogen  
537 and stored at -80°C until further processing was done.

538 The plant material for the seasonal time course study was obtained from 2-year-old branches and apical buds (understood as  
539 the top bud of each branch) of 5-year-old hybrid poplar (*Populus tremula* × *alba* INRA 717 1B4) trees planted at the Centre for  
540 Plant Biotechnology and Genomics (CBGP) in Pozuelo de Alarcón, Madrid (3°49'W, 40°24'N), growing under natural  
541 conditions. Stem samples were collected weekly from November 7, 2014, to April 9, 2015. Buds were collected weekly from  
542 13 January to 14 April 2015. For each time point, stem portions from 8 trees and 25 apical buds from 8 trees were pooled.  
543 RNA extraction was performed using the protocol described in (Ibañez et al. 2008). For the gene expression analysis, the  
544 weekly data were divided into groups named; fall, winter, and spring. Letter suffixes - "a, b, c, d, e" were added to group  
545 names representing "early," "mid," "late", "fortnight-1" or "fortnight-2" based on sampling dates within each season,  
546 following the Northern Meteorological Seasons dates.

547 ***Setaria italica* and *Setaria viridis***. Seeds (*S. italica* B100 and *S. viridis* A10.1) were sown in flats (4x9 inserts/flat) containing  
548 Metro mix 360 soil and grown in a growth chamber, under 12 h day and 12 h night conditions, maintained at 31°C/22°C,  
549 50%-60% humidity; 450  $\mu\text{mol m}^{-2}\text{s}^{-1}$ . Plants were watered once a day or every two days depending on the size of plants and  
550 soil conditions and fertilized twice a week (Tuesday and Friday) using Jack's 15-16-17 at a concentration of 100 ppm. For  
551 light treatment experiments, plants were grown under continuous monochromatic light, blue: 6  $\mu\text{mol m}^{-2}\text{s}^{-1}$ , red: 50  $\mu\text{mol m}^{-2}\text{s}^{-1}$ ,  
552 far-red: 80  $\mu\text{mol m}^{-2}\text{s}^{-1}$ , respectively and watered with RO water every 3 days. Total aerial tissues were collected (at 9.30  
553 AM) from 8-day old seedlings.

554 ***Sorghum bicolor***. The reference line BTx623 was grown under 14 h day greenhouse conditions in topsoil to generate tissue  
555 for two separate experiments: (1) a nitrogen source study and (2) a tissue by developmental stage timecourse. For the  
556 nitrogen source study, plants grown under differing nitrogen source regimes (see *Glycine max*) were harvested at 30 days  
557 after emergence (DAE). For the tissue by developmental stage timecourse, plants were harvested at the juvenile stage (8  
558 DAE), the vegetative stage (24 DAE), at floral initiation (44 DAE), at anthesis (65 DAE), and at grain maturity (96 DAE) and leaf,  
559 root, stem and reproductive structures as described in McCormick et al (McCormick et al. 2017).

560 ***Sorghum bicolor* var Rio**. Genetic material for *S. bicolor* var Rio was obtained from a single seed source provided by W.  
561 Rooney at Texas A&M University. Plants were grown in greenhouse conditions and material for RNA extraction was collected  
562 at 6 biological stages: vegetative (5-leaf), floral initiation, flag leaf, anthesis, soft dough, and hard dough. Stages were  
563 identified based on biological characteristics defined in (Vanderlip and Reeves 1972). At every stage, whole plants were  
564 harvested, and the topmost fully developed leaf and topmost internode were collected. During the first 3 stages, meristems  
565 were isolated from the topmost internode while floral and seed tissues were collected after plants had flowered. All tissues  
566 were immediately placed in RNA Later and stored at 4°C prior to RNA extraction. See also (Cooper et al. 2019).

567 ***Sphagnum angustifolium* (formally *S. fallax*)**. *S. angustifolium* were grown on BCD agar media pH 6.5, ambient temperature  
568 (20°C) and 350  $\mu\text{mol m}^{-2}\text{s}^{-1}$  of photosynthetically active radiation (PAR) at a 12 h light/dark cycle for 2 months prior to  
569 initiation of experimental conditions. At 8 am on the morning of the treatments, *Sphagnum* plantlets were transferred to petri  
570 dishes with 15 ml of appropriate BCD liquid media and placed in a temperature-controlled growth cabinet. Excluding the dark  
571 treatment, all samples were kept under 350 PAR for the duration of the experiment. Morning treatment samples were  
572 harvested at noon. After each experiment the material was blotted dry, placed in a 15 mL Eppendorf tube, flash frozen in  
573 liquid nitrogen, and stored at -80°C until RNA extractions were completed.

574 For the control treatment, *Sphagnum* plants were placed in a 22.05  $\text{cm}^2$  petri dish containing BCD media 6.5 pH and  
575 incubated in a growth cabinet at 20°C and ambient light 350 PAR. To test low pH gene expression, the sample was placed in  
576 a 22.05  $\text{cm}^2$  petri dish containing 6.5 pH BCD media at 8 AM. Each hour, the pH was gradually decreased until the sample  
577 was transferred to 3.5 pH media at 11 AM. The samples were harvested at 12 PM. This treatment was repeated for the high  
578 pH experiment except the sample was gradually brought from 6.5 to 9.0 pH. Temperature experiments were controlled in  
579 growth cabinets plantlets in 22.05  $\text{cm}^2$  petri dishes containing 6.5 pH BCD media. The high temperature treatment began at  
580 20°C and over three hours, temperature was gradually increased to 40°C. The low temperature treatment began at 20°C and

581 over three hours, was gradually decreased to 6°C. To test water loss effects on gene expression, plantlets were placed on dry  
582 plates (no BCD media) for the duration of the experiment. Dark effect on gene expression was tested by placing plant  
583 material in a BCD filled petri dish in complete darkness from 8 AM to 12 PM. To evaluate gene expression that is present  
584 during immature growth stages, a sporophyte was collected from the mother of the *S. angustifolium* pedigree and germinated  
585 on solid Knop medium under axenic tissue culture conditions. After 10 days of growth, plantlets were predominantly within  
586 the thalloid protonemata with rhizoid stage and flash frozen in LN2 until RNA extraction using CTAB lysis buffer and Spectrum  
587 Total Plant RNA kit.  
588

#### 589 **RNA extraction and sequencing**

590 All tissues were immediately flash frozen in liquid nitrogen and stored at -80°C until further processing was done. Every  
591 harvest involved at least three independent biological replicates for each condition. High quality RNA was extracted mainly  
592 using standard Trizol-reagent based extraction (Z. Li and Trick 2005), exceptions noted above under individual species. The  
593 integrity and concentration of the RNA preparations were checked initially using Nano-Drop ND-1000 (Nano-Drop  
594 Technologies) and then by BioAnalyzer (Agilent Technologies). Plate-based RNA sample prep was performed on the  
595 PerkinElmer Sciclone NGS robotic liquid handling system using Illumina's TruSeq Stranded mRNA HT sample prep kit utilizing  
596 poly-A selection of mRNA following the protocol outlined by Illumina in their user guide:  
597 [http://support.illumina.com/sequencing/sequencing\\_kits/truseq\\_stranded\\_mrna\\_ht\\_sample\\_prep\\_kit.html](http://support.illumina.com/sequencing/sequencing_kits/truseq_stranded_mrna_ht_sample_prep_kit.html), and with the  
598 following conditions: total RNA starting material was 1 µg per sample and 8 cycles of PCR was used for library amplification.  
599 The prepared libraries were then quantified by qPCR using the Kapa SYBR Fast Illumina Library Quantification Kit (Kapa  
600 Biosystems) and run on a Roche LightCycler 480 real-time PCR instrument. The quantified libraries were then prepared for  
601 sequencing on the Illumina HiSeq sequencing platform utilizing a TruSeq paired-end cluster kit, v4, and Illumina's cBot  
602 instrument to generate a clustered flow cell for sequencing. Sequencing of the flow cell was performed on the Illumina  
603 HiSeq2500 sequencer using HiSeq TruSeq SBS sequencing kits, v4, following a 2x150 indexed run recipe. The same  
604 standardized protocols were used to prevent introduction of any batch effects among samples throughout the project.  
605

#### 606 **RNA-seq data normalization and differential gene expression analysis**

607 Illumina RNA-seq 150 bp paired-end strand-specific reads were processed using custom Python scripts to trim adapter  
608 sequences and low-quality bases to obtain high quality ( $Q \geq 25$ ) sequence data. Reads shorter than 50 bp after trimming were  
609 discarded. The processed high-quality RNA-seq reads were aligned to current reference genomes of Gene Atlas using  
610 GSNAP, a short read alignment program (Wu and Nacu 2010). HTSeq v1.99.2, a Python package was used to count reads  
611 mapped to annotated genes in the reference genome (Anders, Pyl, and Huber 2015).

612 Multiple steps for vetting libraries and identifying outliers were employed, including visualizing the multidimensional scaling  
613 plots to identify batch effects, if any, and outliers among the biological replicates were further identified based on Euclidean  
614 distance to the cluster center and the Pearson correlation coefficient,  $r \geq 0.85$ . Libraries retained after QC and outlier-filtering  
615 steps were only considered for further analysis. Detected batch effects, if any, were accounted for using RUVSeq (v1.4.0)  
616 (Risso et al. 2014) with the residual RUVr approach. Fragments per kilobase of exon per million fragments mapped (FPKM)  
617 and transcripts per million (TPM) values were calculated for each gene by normalizing the read count data to both the length  
618 of the gene and the total number of mapped reads in the sample and considered as the metric for estimating gene expression  
619 levels (B. Li and Dewey 2011; Trapnell et al. 2011). Genes with low expression were filtered out, by requiring  $\geq 2$  relative log  
620 expression normalized counts in at least two samples for each gene. Differential gene expression analysis was performed  
621 using the DESeq2 package (v1.30.1) (Love, Huber, and Anders 2014) with adjusted  $P$ -value  $< 0.05$  using the Benjamini &  
622 Hochberg method and an  $\log_2$  fold change  $> 1$  as the statistical cutoff for differentially expressed genes.  
623

#### 624 **Co-expression network construction**

625 Weighted gene co-expression networks were constructed using the WGCNA R package (v1.70.3) (Langfelder and Horvath  
626 2008) with normalized expression data retained after filtering genes showing low expression levels ( $\log_2$  values of expression  
627  $< 2$ ). Subsets of samples belonging to specific experiments such as N study, developmental stages, or stress treatment, were  
628 used to construct multiple networks for each species. Subsetting samples reduces the noise and increases the functional  
629 connectivity and specificity within modules. We followed standard WGCNA network construction procedures for this analysis.  
630 Briefly, pairwise Pearson correlations between each gene pair was weighted by raising them to power ( $\beta$ ). To select proper  
631 soft-thresholding power, the network topology for a range of powers was evaluated and appropriate power was chosen that  
632 ensured an approximate scale-free topology of the resulting network. The pairwise weighted matrix was transformed into a  
633 topological overlap measure (TOM). And the TOM-based dissimilarity measure ( $1 - \text{TOM}$ ) was used for hierarchical clustering  
634 and initial module assignments were determined by using a dynamic tree-cutting algorithm. Pearson correlations between  
635 each gene and each module eigengene, referred to as a gene's module membership, were calculated and module eigengene  
636 distance threshold of 0.25 was used to merge highly similar modules. These co-expression modules were assessed to  
637 determine their association with expression patterns distinct to a tissue or condition. Module eigengenes were associated  
638 with tissues or treatment conditions or developmental stages to gain insight into the role each module might play. These  
639 modules were visualized using igraph R package (v.1.2.6) (Gabor Csardi and Tamas Nepusz 2006) and in order to focus on  
640 relevant gene pair relationships, network depictions were limited to top 500 within-module gene-gene interactions as  
641 measured by topological overlap.  
642

#### 643 **GO and KEGG pathway enrichment analysis**

644 GO enrichment analysis of DEGs, co-expression modules and genes in tissue and condition specific clusters was performed  
645 using topGO (v.2.42.0) (Alexa A and Rahnenfuhrer J 2016), an R Bioconductor package, to determine overrepresented GO  
646 categories across biological process (BP), cellular component (CC) and molecular function (MF) domains. Enrichment of GO  
647 terms was tested using Fisher's exact test with  $P < 0.05$  considered as significant. KEGG (Kanehisa and Goto 2000) pathway

648 enrichment analysis was also performed on those gene sets based on hypergeometric distribution tests and pathways with  $P$   
649 <0.05 were considered as enriched.  
650

#### 651 **Categorization of function descriptions**

652 An augmented dictionary lookup approach that incorporates weighting for positive (amplifiers), negative (including  
653 attenuators), and adversative keywords was adapted from sentiment analysis methodology to categorize gene function  
654 descriptions. We generated a custom dictionary from gene function descriptions of all Gene Atlas plants and used a modified  
655 valence shifters data table with sentimentr (v2.9.0) (<https://cran.r-project.org/web/packages/sentimentr>), to obtain sentiment  
656 score. We empirically determined the minimum cutoff for sentiment score to classify gene descriptions as good (score > 0.3)  
657 and poor (score < 0.3) function descriptors.  
658

#### 659 **Identification of orthologous genes**

660 OrthoFinder (v2.5.4) was used to identify orthologous genes across 18 Gene Atlas species using default parameters (Emms  
661 and Kelly 2019). OrthoFinder results were parsed to generate tables of orthologs for each species and genes with one-to-one  
662 ortholog relationships between species identified using rooted gene trees were further subsetted.  
663

#### 664 **Gene ranking method**

665 To rank and prioritize genes by their biological relevance, genes with distinct expression patterns identified based on i)  
666 tissue/condition specificity, ii) unique DE in a single contrast were given a score of 2 for each method i.e., a gene was  
667 assigned a score of 4 if it were identified by two methods. These scores were augmented with co-expression network  
668 analysis (described above). Genes in biologically relevant modules were ranked (score=2) while hub genes in a co-expression  
669 module were ranked the highest (score=4). Also, gene orthologs with consensus expression pattern in two or more plants  
670 were given additional scores based on the phylogenetic distance between species (Zeng et al. 2014; Kumar et al. 2017) i.e.,  
671 larger the divergence time higher the score (million years ago/100) (**Supplemental Data 16**). Final ranking of the genes was  
672 calculated as the aggregate of individual scores.  
673

#### 674 **System design and implementation**

675 All statistical analyses and visualizations were performed using the R 4.0.3 Statistical Software (R Development Core Team  
676 2011) and its web interface was developed using shiny (v1.7.1). Currently, Gene Atlas is deployed on a CentOS Linux server  
677 by employing Docker (version 19.03.11), an open platform for developing and running applications.  
678

#### 679 **Data availability**

680 The RNA-seq data that support the findings of this study are available from the NCBI Sequence Read Archive (SRA) under  
681 accessions provided in **Supplemental Data 1**. To enable exploration of the transcriptome datasets for JGI Plant Gene Atlas  
682 v2.0, the data are hosted on Gene Atlas portal (<https://plantgeneatlas.jgi.doe.gov>) and JGI's Phytozome plant portal.  
683 Documentation for data processing and downloadable data are available in the 'Methods' section  
684 (<https://plantgeneatlas.jgi.doe.gov>).  
685

#### 686 **Competing financial interests**

687 The authors declare no competing financial interests.  
688

#### 689 **Correspondence and requests for materials** should be addressed to A.S. or J.S. 690

#### 691 **ACKNOWLEDGMENTS**

692 The work (proposal: 10.46936/10.25585/60000843) conducted by the U.S. Department of Energy Joint Genome Institute  
693 (<https://ror.org/04xm1d337>), a DOE Office of Science User Facility, is supported by the Office of Science of the U.S.  
694 Department of Energy operated under Contract No. DE-AC02-05CH11231.  
695

696 The *Populus* work was partially supported by the U.S. Department of Energy under Contract to Oak Ridge National  
697 Laboratory. Oak Ridge National Laboratory is managed by UT-Battelle, LLC for the US Department of Energy under contract  
698 number DE- AC05-00OR22725. Specific funding for the soybean transcriptome atlas was provided by a grant from the  
699 United Soybean Board (to GS). The switchgrass work was carried out under the support of the BioEnergy Science Center  
700 (BESC, a U.S. Department of Energy Bioenergy Research Center supported by the Office of Biological and Environmental  
701 Research in the DOE Office of Science, U.S. Department of Energy) and funded by the Samuel Roberts Noble Foundation. BH  
702 work was funded in part by U.S. DOE the Office of Biological and Environmental Research under grant number DE-  
703 SC0012629. The *Chlamydomonas* work is supported by the US Department of Energy Grant DE-FC02-02ER63421 and by the  
704 National Institutes of Health (NIH) R24 GM092473 to SM. The Eucalyptus work was supported by the Brazilian Federal District  
705 Research Foundation (FAP-DF) NEXTREE grant. The *Panicum hallii* work was supported by the DOE Office of Science, Office  
706 of Biological and Environmental Research (BER), grant no. DE-SC0008451 and DE-SC0021126 to TEJ. The sorghum work by  
707 JM laboratory was funded in part by the DOE Great Lakes Bioenergy Research Center (DOE BER grant DE-SC0018409). The  
708 *Setaria* work was funded by the DOE Office of Science under grant numbers DE-SC0018277 and DE-SC0008769. The  
709 *Kalanchoe* work was partially supported by the DOE Office of Science, Genomic Science Program under Award No. DE-  
710 SC0008834. Research related to Sphagnum was funded by DOE BER Early Career Research Program at Oak Ridge National  
711 Laboratory.  
712

714 Laboratory is managed by UT-Battelle, LLC, for the US DOE under contract number DE-AC05-00OR22725. Thanks to Daniel  
715 S. Rokhsar for involvement in the early formulation of Gene Atlas and helpful discussions.  
716

## 717 **AUTHOR CONTRIBUTIONS**

718 A.S. and C.P. conducted transcriptome data analyses. J.T.L. conducted metadata analysis. M.S.H. carried out soybean and  
719 *Medicago* experiments. J.G., K.B., M.A., M.K., M.W., A.L., Jenifer J., L.S., K.A., M.Z., C.D. performed RNA-seq library  
720 preparation and sequencing. J.K. and S.D.G. conducted *Chlamydomonas* experiments. J.C., J.P., and D.G. maintains the  
721 data repository at Phytozome. J.W.J. and C.P. assembled genomes. S.S. conducted genome annotation at JGI. I.T-J., and  
722 M.U. conducted *Panicum virgatum* experiments. S.S.J. conducted *Populus* experiments and *Sphagnum* RNA extractions.  
723 D.C. and M.P. conducted *Populus* seasonal time course experiments. H.J., C.S., P.H., J.S., C.L., A.M. and S.C. conducted  
724 *Setaria* experiments and sample preparations. L.L. conducted *Brachypodium* cold treatment experiments. A.A.C. conducted  
725 *Sphagnum* experiments. B.W. conducted *Sorghum* N-treatment experiments. R.H. conducted *Kalanchoe* experiments. M.R.P.  
726 conducted *Eucalyptus* experiments. R.T. and K.S. conducted validation experiments for N-treatment. E.V.S. and X.W.  
727 conducted *Arabidopsis*, *P. hallii* and *P. virgatum* photoperiod experiments and sample preparations. A.M. conducted *P.*  
728 *virgatum* drought stress experiments and sample preparation. P.F.P. and F.B.H. analyzed *Physcomitrium* data. P.F.P., M.H.  
729 and S.A.R. provided *Physcomitrium* samples. D.S.R., D.G., D.T., D.W., E.A.C., E.K., G.S., G.A.T., I.B., J.S., J.M., J.V., S.A.R.,  
730 S.S.M., T.B., T.E.J., T.C.M., X.Y., and Y.T. are principal investigators (alphabetical order). All authors read and approved the  
731 final manuscript.  
732 A.S., J.T.L., and J.S. prepared the manuscript with input from all authors.  
733  
734

## 735 **SUPPLEMENTAL MATERIAL**

736 **Supplemental Data 1.** Correlation among biological replicates in Gene Atlas species.

737 **Supplemental Data 2.** RNA-seq samples generated/analyzed in this study.

738 **Supplemental Data 3.** One-to-one orthologous genes across eight vascular plants.

739 **Supplemental Data 4.** One-to-one orthologous genes with consistent expression among species, but weak functional  
740 descriptions.

741 **Supplemental Data 5.** *Arabidopsis thaliana* (TAIR10) orthologs of genes with conserved expression patterns across Gene  
742 Atlas plants.

743 **Supplemental Data 6.** Percentage of genes commonly expressed in multiple tissues in Gene Atlas plants.

744 **Supplemental Data 7.** Genes with strong expression proclivity towards selected tissues/conditions in *G. max*, *P. patens* and  
745 *S. angustifolium*.

746 **Supplemental Data 8.** Genes with strong tissue/condition specific expression across Gene Atlas plants.

747 **Supplemental Data 9.** Overrepresented biological processes among genes with strong tissue/condition specific expression.

748 **Supplemental Data 10.** Differentially expressed genes in nitrogen treatment study.

749 **Supplemental Data 11.** Co-expression network module genes generated across different sets of tissues and conditions  
750 within Gene Atlas plants.

751 **Supplemental Data 12.** Overrepresented biological processes among co-expression network module gene sets generated  
752 across different sets of tissues and conditions within Gene Atlas plants.

753 **Supplemental Data 13.** List of hub genes in co-expression network modules.

754 **Supplemental Data 14.** Expression derived function descriptions (EDFD) assigned to annotated genes across Gene Atlas  
755 plants.

756 **Supplemental Data 15.** Prioritized top ranked genes with poor functional descriptions for future experimental investigations.

757 **Supplemental Data 16.** Estimates of divergence time between Gene Atlas species.

758

759

## 760 **REFERENCES**

761 Alexa A and Rahnenfuhrer J. 2016. "topGO: Enrichment Analysis for Gene Ontology." R Package Version 2.24.0. 2016.  
762 <http://bioconductor.org/packages/release/bioc/html/topGO.html>.

763 Anders, Simon, Paul Theodor Pyl, and Wolfgang Huber. 2015. "HTSeq-A Python Framework to Work with High-Throughput  
764 Sequencing Data." *Bioinformatics* 31 (2): 166–69.

765 Berardini, Tanya Z., Leonore Reiser, Donghui Li, Yarik Mezheritsky, Robert Muller, Emily Strait, and Eva Huala. 2015. "The  
766 Arabidopsis Information Resource: Making and Mining the 'Gold Standard' Annotated Reference Plant Genome."

767         *Genesis* 53 (8): 474–85.

768     Bruex, Angela, Raghunandan M. Kainkaryam, Yana Wieckowski, Yeon Hee Kang, Christine Bernhardt, Yang Xia, Xiaohua  
769         Zheng, et al. 2012. “A Gene Regulatory Network for Root Epidermis Cell Differentiation in *Arabidopsis*.” *PLoS Genetics*  
770         8 (1). <https://doi.org/10.1371/journal.pgen.1002446>.

771     Canales, Javier, Tomás C. Moyano, Eva Villarroel, and Rodrigo A. Gutiérrez. 2014. “Systems Analysis of Transcriptome Data  
772         Provides New Hypotheses about *Arabidopsis* Root Response to Nitrate Treatments.” *Frontiers in Plant Science* 5: 22.

773     Cooper, Elizabeth A., Zachary W. Brenton, Barry S. Flinn, Jerry Jenkins, Shengqiang Shu, Dave Flowers, Feng Luo, et al.  
774         2019. “A New Reference Genome for Sorghum Bicolor Reveals High Levels of Sequence Similarity between Sweet and  
775         Grain Genotypes: Implications for the Genetics of Sugar Metabolism.” *BMC Genomics* 20 (1): 420.

776     Cove, David J., Pierre-François Perroud, Audra J. Charron, Stuart F. McDaniel, Abha Khandelwal, and Ralph S. Quatrano.  
777         2009. “The Moss *Physcomitrella Patens*: A Novel Model System for Plant Development and Genomic Studies.” *Cold  
778         Spring Harbor Protocols* 2009 (2): db.em0115.

779     Emms, David M., and Steven Kelly. 2019. “OrthoFinder: Phylogenetic Orthology Inference for Comparative Genomics.”  
780         *Genome Biology* 20 (1): 238.

781     Faye, Jacques M., Eyanawa A. Akata, Bassirou Sine, Cyril Diatta, Ndiaga Cisse, Daniel Fonceka, and Geoffrey P. Morris.  
782         2022. “Quantitative and Population Genomics Suggest a Broad Role of Stay-Green Loci in the Drought Adaptation of  
783         Sorghum.” *The Plant Genome* 15 (1): e20176.

784     Fernandez-Pozo, N., F. B. Haas, R. Meyberg, K. K. Ullrich, M. Hiss, P-F Perroud, S. Hanke, et al. 2020. “PEATmoss  
785         (*Physcomitrella Expression Atlas Tool*): A Unified Gene Expression Atlas for the Model Plant *Physcomitrella Patens*.”  
786         *The Plant Journal: For Cell and Molecular Biology* 102 (1). <https://doi.org/10.1111/tpj.14607>.

787     Gabor Csardi and Tamas Nepusz. 2006. “The Igraph Software Package for Complex Network Research.” *InterJournal*,  
788         Complex Systems. 2006. <http://igraph.org>.

789     Gelli, Malleswari, Yongchao Duo, Anji Konda, Chi Zhang, David Holding, Ismail Dweikat, A. B. Maunder, et al. 2014.  
790         “Identification of Differentially Expressed Genes between Sorghum Genotypes with Contrasting Nitrogen Stress  
791         Tolerance by Genome-Wide Transcriptional Profiling.” *BMC Genomics* 15 (1): 179.

792     Ghazalpour, Anatole, Sudheer Doss, Bin Zhang, Susanna Wang, Christopher Plaisier, Ruth Castellanos, Alec Brozell, et al.  
793         2006. “Integrating Genetic and Network Analysis to Characterize Genes Related to Mouse Weight.” *PLoS Genetics* 2  
794         (8): e130.

795     Gollery, Martin, Jeff Harper, John Cushman, Taliah Mittler, Thomas Girke, Jian-Kang Zhu, Julia Bailey-Serres, et al. 2006.  
796         “What Makes Species Unique? The Contribution of Proteins with Obscure Features.” *Genome Biology* 7 (7): R57.

797     Gollery, Martin, Jeff Harper, John Cushman, Taliah Mittler, and Ron Mittler. 2007. “POFs: What We Don’t Know Can Hurt Us.”  
798         *Trends in Plant Science* 12 (11): 492–96.

799     Goodstein, David M., Shengqiang Shu, Russell Howson, Rochak Neupane, Richard D. Hayes, Joni Fazo, Therese Mitros, et  
800         al. 2012. “Phytozome: A Comparative Platform for Green Plant Genomics.” *Nucleic Acids Research* 40 (D1): 1–9.

801     Horvath, S., B. Zhang, M. Carlson, K. V. Lu, S. Zhu, R. M. Felciano, M. F. Laurance, et al. 2006. “Analysis of Oncogenic  
802         Signaling Networks in Glioblastoma Identifies *ASPM* as a Molecular Target.” *Proceedings of the National Academy of  
803         Sciences of the United States of America* 103 (46): 17402–7.

804     Huang, Jianyan, Xiaobo Zhao, and Joanne Chory. 2019. “The *Arabidopsis* Transcriptome Responds Specifically and  
805         Dynamically to High Light Stress.” *Cell Reports* 29 (12): 4186–99.e3.

806     Hufnagel, Bárbara, André Marques, Alexandre Soriano, Laurence Marquès, Fanchon Divol, Patrick Doumas, Erika Sallet, et al.  
807         2020. “High-Quality Genome Sequence of White Lupin Provides Insight into Soil Exploration and Seed Quality.” *Nature  
808         Communications*. <https://doi.org/10.1038/s41467-019-14197-9>.

809     Ibañez, Cristian, Alberto Ramos, Paloma Acebo, Angela Contreras, Rosa Casado, Isabel Allona, and Cipriano Aragoncillo.  
810         2008. “Overall Alteration of Circadian Clock Gene Expression in the Chestnut Cold Response.” *PloS One* 3 (10): e3567.

811     Inglis, Peter W., Marilia de Castro R. Pappas, Lucileide V. Resende, and Dario Grattapaglia. 2018. “Fast and Inexpensive  
812         Protocols for Consistent Extraction of High Quality DNA and RNA from Challenging Plant and Fungal Samples for High-  
813         Throughput SNP Genotyping and Sequencing Applications.” *PloS One* 13 (10): e0206085.

814     Jin, Jinpu, Feng Tian, De-Chang Yang, Yu-Qi Meng, Lei Kong, Jingchu Luo, and Ge Gao. 2017. “PlantTFDB 4.0: Toward a  
815         Central Hub for Transcription Factors and Regulatory Interactions in Plants.” *Nucleic Acids Research* 45 (D1): D1040–  
816         45.

817     Kanehisa, M., and S. Goto. 2000. “KEGG: Kyoto Encyclopedia of Genes and Genomes.” *Nucleic Acids Research* 28 (1): 27–  
818         30.

819     Keightley, Peter D., and William George Hill. 1990. “Variation Maintained in Quantitative Traits with Mutation-selection

820        Balance: Pleiotropic Side-Effects on Fitness Traits." *Proceedings of the Royal Society of London. Series B: Biological Sciences* 242 (1304): 95–100.

821

822        Kogawara, Satoshi, Takashi Yamanoshita, Mariko Norisada, and Katsumi Kojima. 2014. "Steady Sucrose Degradation Is a Prerequisite for Tolerance to Root Hypoxia." *Tree Physiology* 34 (3): 229–40.

823

824        Koornneef, Maarten, and David Meinke. 2010. "The Development of Arabidopsis as a Model Plant." *The Plant Journal: For Cell and Molecular Biology* 61 (6): 909–21.

825

826        Kryuchkova-Mostacci, Nadezda, and Marc Robinson-Rechavi. 2017. "A Benchmark of Gene Expression Tissue-Specificity Metrics." *Briefings in Bioinformatics* 18 (2): 205–14.

827

828        Kumar, Sudhir, Glen Stecher, Michael Suleski, and S. Blair Hedges. 2017. "TimeTree: A Resource for Timelines, Timetrees, and Divergence Times." *Molecular Biology and Evolution* 34 (7): 1812–19.

829

830        Langfelder, Peter, and Steve Horvath. 2008. "WGCNA: An R Package for Weighted Correlation Network Analysis." *BMC Bioinformatics* 9 (January): 559.

831

832        Levin, J. Z., M. Yassour, X. Adiconis, C. Nusbaum, D. A. Thompson, N. Friedman, A. Gnirke, and A. Regev. 2010. "Comprehensive Comparative Analysis of Strand Specific RNA Sequencing Methods." *Nature Methods* 7 (9): 709–15.

833

834        Li, Bo, and Colin N. Dewey. 2011. "RSEM: Accurate Transcript Quantification from RNA-Seq Data with or without a Reference Genome." *BMC Bioinformatics* 12 (1): 323.

835

836        Li, Chun, Qi Gang Li, Jim M. Dunwell, and Yuan Ming Zhang. 2012. "Divergent Evolutionary Pattern of Starch Biosynthetic Pathway Genes in Grasses and Dicots." *Molecular Biology and Evolution* 29 (10): 3227–36.

837

838        Liu, Wenwen, Guangming He, and Xing Wang Deng. 2021. "Biological Pathway Expression Complementation Contributes to Biomass Heterosis in Arabidopsis." *Proceedings of the National Academy of Sciences of the United States of America* 118 (16): e2023278118.

839

840

841        Li, W., P. Lan, and 3.948. 2015. "Re-Analysis of RNA-Seq Transcriptome Data Reveals New Aspects of Gene Activity in Arabidopsis Root Hairs." *Frontiers in Plant Science* 6 (June): 421.

842

843        Li, Yinruizhi, Mengdi Wang, Ke Teng, Di Dong, Zhuocheng Liu, Tiejun Zhang, and Liebao Han. 2022. "Transcriptome Profiling Revealed Candidate Genes, Pathways and Transcription Factors Related to Nitrogen Utilization and Excessive Nitrogen Stress in Perennial Ryegrass." *Scientific Reports* 12 (1): 3353.

844

845

846        Li, Zhiwu, and Harold N. Trick. 2005. "Rapid Method for High-Quality RNA Isolation from Seed Endosperm Containing High Levels of Starch." *BioTechniques* 38 (6): 872, 874, 876.

847

848        Loreti, Elena, Alessandra Poggi, Giacomo Novi, Amedeo Alpi, and Pierdomenico Perata. 2005. "A Genome-Wide Analysis of the Effects of Sucrose on Gene Expression in Arabidopsis Seedlings under Anoxia." *Plant Physiology* 137 (3): 1130–38.

849

850        Love, Michael I., Wolfgang Huber, and Simon Anders. 2014. "Moderated Estimation of Fold Change and Dispersion for RNA-Seq Data with DESeq2." *Genome Biology* 15 (12): 550.

851

852        Ma, Fei, Lijuan Wang, Jiale Li, Muhammad Kaleem Samma, Yanjie Xie, Ren Wang, Jin Wang, Jing Zhang, and Wenbiao Shen. 2014. "Interaction between HY1 and H2O2 in Auxin-Induced Lateral Root Formation in Arabidopsis." *Plant Molecular Biology* 85 (1-2): 49–61.

853

854

855        Manzano, Concepción, Mercedes Pallero-Baena, Ilda Casimiro, Bert De Rybel, Beata Orman-Ligeza, Gert Van Isterdael, Tom Beeckman, Xavier Draye, Pedro Casero, and Juan C. Del Pozo. 2014. "The Emerging Role of Reactive Oxygen Species Signaling during Lateral Root Development." *Plant Physiology* 165 (3): 1105–19.

856

857

858        McCormick, R. F., S. K. Truong, A. Sreedasyam, J. Jenkins, S. Shu, D. Sims, M. Kennedy, et al. 2017. "The Sorghum Bicolor Reference Genome: Improved Assembly, Gene Annotations, a Transcriptome Atlas, and Signatures of Genome Organization." *The Plant Journal: For Cell and Molecular Biology*. <https://doi.org/10.1111/tpj.13781>.

859

860

861        Miller, Jeremy A., Michael C. Oldham, and Daniel H. Geschwind. 2008. "A Systems Level Analysis of Transcriptional Changes in Alzheimer's Disease and Normal Aging." *The Journal of Neuroscience: The Official Journal of the Society for Neuroscience* 28 (6): 1410–20.

862

863

864        Mukhtar, M. Shahid, Anne-Ruxandra Carvunis, Matija Dreze, Petra Epple, Jens Steinbrenner, Jonathan Moore, Murat Tasan, et al. 2011. "Independently Evolved Virulence Effectors Converge onto Hubs in a Plant Immune System Network." *Science* 333 (6042): 596–601.

865

866

867        Nicotra, A. B., O. K. Atkin, S. P. Bonser, A. M. Davidson, E. J. Finnegan, U. Mathesius, P. Poot, et al. 2010. "Plant Phenotypic Plasticity in a Changing Climate." *Trends in Plant Science*. <https://doi.org/10.1016/j.tplants.2010.09.008>.

868

869        Passaia, Gisele, Guillaume Queval, Juan Bai, Marcia Margis-Pinheiro, and Christine H. Foyer. 2014. "The Effects of Redox Controls Mediated by Glutathione Peroxidases on Root Architecture in Arabidopsis Thaliana." *Journal of Experimental Botany* 65 (5): 1403–13.

870

871

872        Peña, Maria J., Yingzhen Kong, William S. York, and Malcolm A. O'Neill. 2012. "A Galacturonic Acid-Containing Xyloglucan Is

873         Involved in Arabidopsis Root Hair Tip Growth." *The Plant Cell* 24 (11): 4511–24.

874     Perroud, Pierre-François, Fabian B. Haas, Manuel Hiss, Kristian K. Ullrich, Alessandro Alboresi, Mojgan Amirebrahimi, Kerrie  
875     Barry, et al. 2018. "The Physcomitrella Patens Gene Atlas Project: Large-Scale RNA-Seq Based Expression Data." *The  
876     Plant Journal: For Cell and Molecular Biology* 95 (1): 168–82.

877     Raissig, Michael T., Juliana L. Matos, M. Ximena Anleu Gil, Ari Kornfeld, Akhila Bettadapur, Emily Abrash, Hannah R. Allison,  
878     et al. 2017. "Mobile MUTE Specifies Subsidiary Cells to Build Physiologically Improved Grass Stomata." *Science* 355  
879     (6330): 1215–18.

880     Reski, R., and W. O. Abel. 1985. "Induction of Budding on Chloronemata and Caulonemata of the Moss, Physcomitrella  
881     Patens, Using Isopentenyladenine." *Planta* 165 (3): 354–58.

882     Rhee, Seung Yon, and Marek Mutwil. 2014. "Towards Revealing the Functions of All Genes in Plants." *Trends in Plant  
883     Science* 19 (4): 212–21.

884     Risso, Davide, John Ngai, Terence P. Speed, and Sandrine Dudoit. 2014. "Normalization of RNA-Seq Data Using Factor  
885     Analysis of Control Genes or Samples (RUVSeq)." *Nature Biotechnology* 32 (9): 896–902.

886     Ross, Michael G., Carsten Russ, Maura Costello, Andrew Hollinger, Niall J. Lennon, Ryan Hegarty, Chad Nusbaum, et al.  
887     2013. "Characterizing and Measuring Bias in Sequence Data." *Genome Biology* 14 (5): R51.

888     Somssich, Marc, Ghazanfar Abbas Khan, and Staffan Persson. 2016. "Cell Wall Heterogeneity in Root Development of  
889     Arabidopsis." *Frontiers in Plant Science* 7 (August): 1242.

890     Sudmant, Peter H., Maria S. Alexis, and Christopher B. Burge. 2015. "Meta-Analysis of RNA-Seq Expression Data across  
891     Species, Tissues and Studies." *Genome Biology* 16 (1): 287.

892     Swift, Joseph, Jose M. Alvarez, Viviana Araus, Rodrigo A. Gutiérrez, and Gloria M. Coruzzi. 2020. "Nutrient Dose-Responsive  
893     Transcriptome Changes Driven by Michaelis-Menten Kinetics Underlie Plant Growth Rates." *Proceedings of the  
894     National Academy of Sciences* 117 (23): 12531–40.

895     Torkamani, Ali, Brian Dean, Nicholas J. Schork, and Elizabeth A. Thomas. 2010. "Coexpression Network Analysis of Neural  
896     Tissue Reveals Perturbations in Developmental Processes in Schizophrenia." *Genome Research* 20 (4): 403–12.

897     Trapnell, Cole, Brian a. Williams, Geo Pertea, Ali Mortazavi, Gordon Kwan, Marijke J. van Baren, Steven L. Salzberg, Barbara  
898     J. Wold, and Lior Pachter. 2011. "Transcript Assembly and Abundance Estimation from RNA-Seq Reveals Thousands  
899     of New Transcripts and Switching among Isoforms." *Nature Biotechnology* 28 (5): 511–15.

900     Vanderlip, R. L., and H. E. Reeves. 1972. "Growth Stages of Sorghum [ *Sorghum Bicolor* , (L.) Moench.]<sup>1</sup>." *Agronomy Journal*  
901     64 (1): 13–16.

902     Voineagu, Irina, Xinchen Wang, Patrick Johnston, Jennifer K. Lowe, Yuan Tian, Steve Horvath, Jonathan Mill, Rita M. Cantor,  
903     Benjamin J. Blencowe, and Daniel H. Geschwind. 2011. "Transcriptomic Analysis of Autistic Brain Reveals Convergent  
904     Molecular Pathology." *Nature* 474 (7351): 380–84.

905     Wu, Thomas D., and Serban Nacu. 2010. "Fast and SNP-Tolerant Detection of Complex Variants and Splicing in Short  
906     Reads." *Bioinformatics* 26 (7): 873–81.

907     Yanai, Itai, Hila Benjamin, Michael Shmoish, Vered Chalifa-Caspi, Maxim Shklar, Ron Ophir, Arren Bar-Even, et al. 2005.  
908     "Genome-Wide Midrange Transcription Profiles Reveal Expression Level Relationships in Human Tissue Specification."  
909     *Bioinformatics* 21 (5): 650–59.

910     Yu, Y., J. C. Fuscoe, C. Zhao, C. Guo, M. Jia, T. Qing, D. I. Bannon, et al. 2014. "A Rat RNA-Seq Transcriptomic BodyMap  
911     across 11 Organs and 4 Developmental Stages." *Nature Communications* 5: 3230.

912     Zeng, Liping, Qiang Zhang, Renran Sun, Hongzhi Kong, Ning Zhang, and Hong Ma. 2014. "Resolution of Deep Angiosperm  
913     Phylogeny Using Conserved Nuclear Genes and Estimates of Early Divergence Times." *Nature Communications* 5  
914     (September): 4956.

915     Zhang, Fei, Jinfeng Wu, Nir Sade, Si Wu, Aiman Egbaria, Alisdair R. Fernie, Jianbing Yan, et al. 2021. "Genomic Basis  
916     Underlying the Metabolome-Mediated Drought Adaptation of Maize." *Genome Biology* 22 (1): 260.

917

918

919

920

921

922

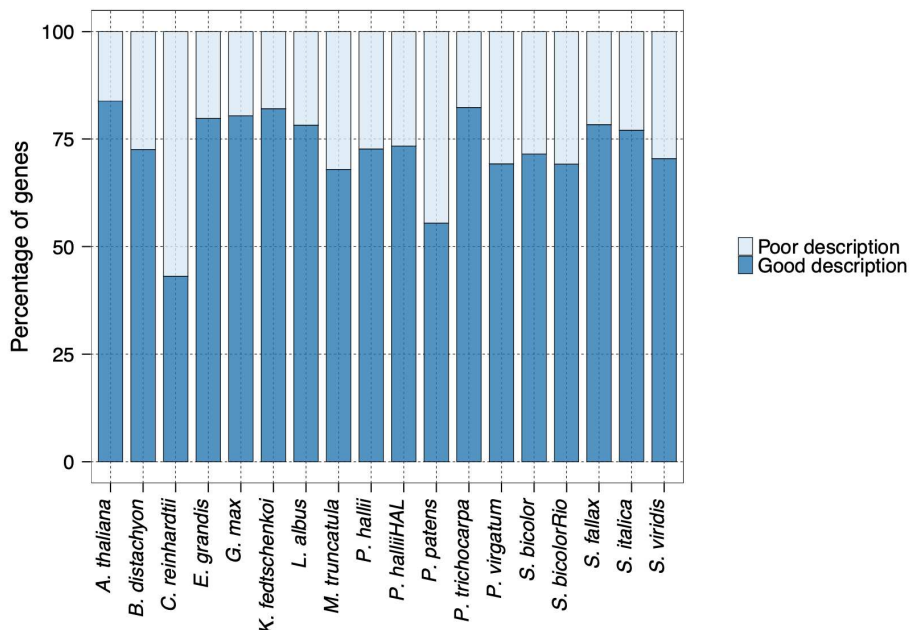
923

924

925

## 926 SUPPLEMENTAL FIGURES

927



928

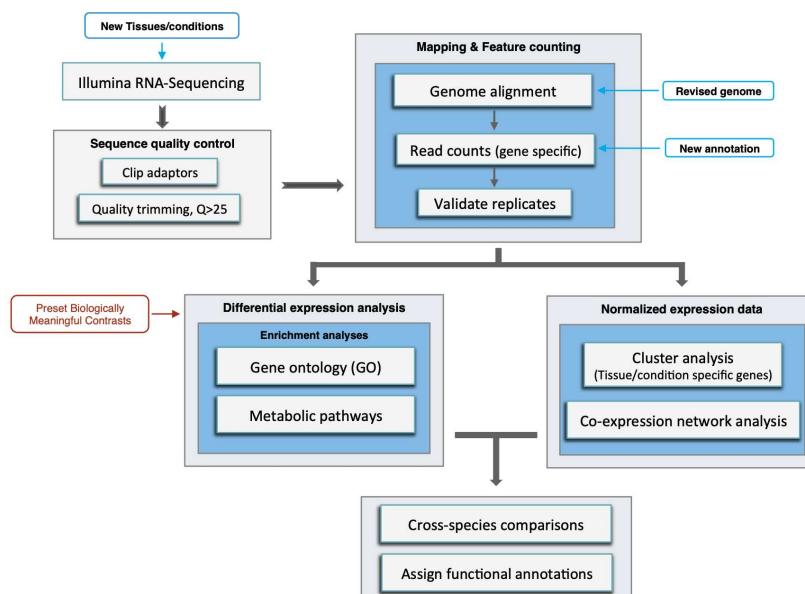
929

**930 Supplemental Figure 1 | Classification of gene function descriptions.** Percentage of genes with poor and good function  
931 descriptions categorized using an augmented dictionary lookup approach that incorporates weighting for negative, positive and  
932 adversative keywords.

933

934

935



936

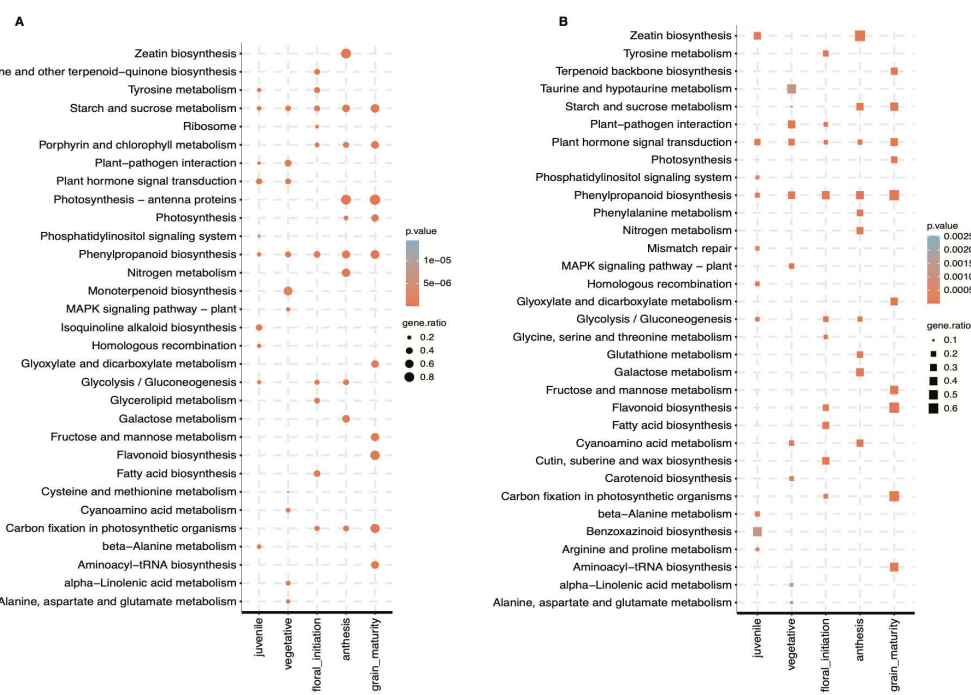
937

938

939

**937 Supplemental Figure 2 | Plant Gene Atlas analysis flowchart.** Pipeline representing methodology used to analyze RNA-seq  
938 data and assign experimentally derived functional annotations.

940



941

**Supplemental Figure 3 | Differentially expressed gene comparison across five developmental stages in *Sorghum bicolor*.** Top 10 KEGG metabolic pathway enrichments ( $P < .05$ , hypergeometric test) of down-regulated differentially expressed genes in each of the five developmental stages (A) and down-regulated genes unique to each stage (B). 'gene.ratio' represents the ratio of number of DEGs over the number of genes annotated specific to the pathway.

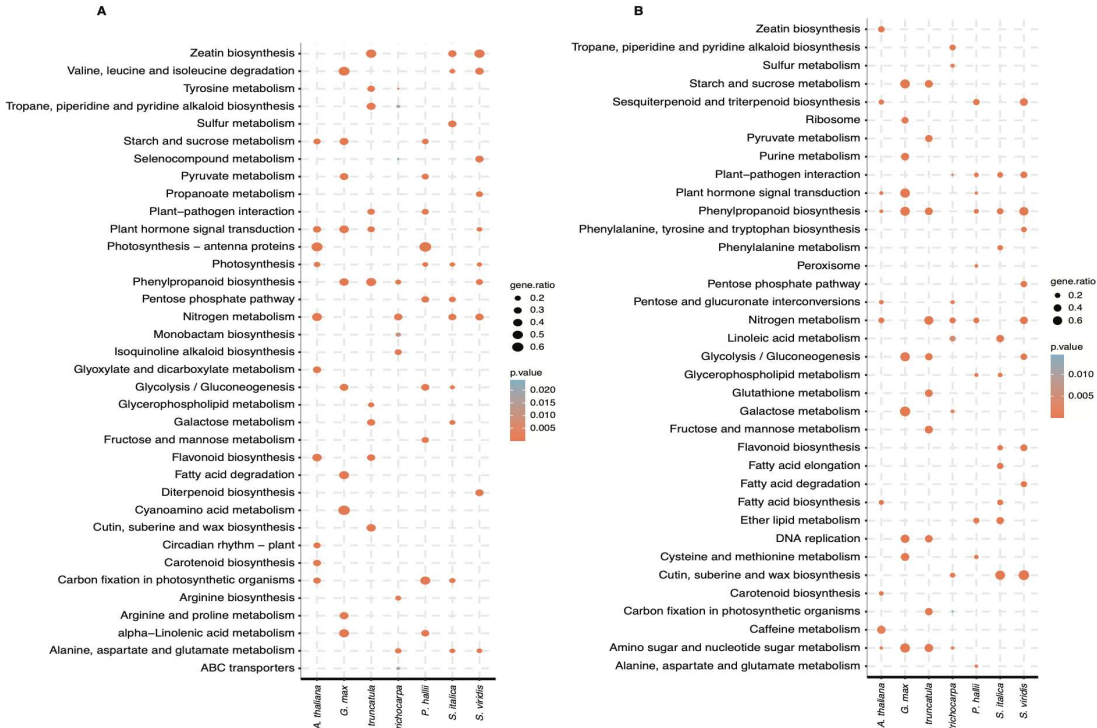
942

943

944

945

946



947

948

949

**Supplemental Figure 4 | Transcriptional response of Gene Atlas plants towards  $\text{NH}_4^+$  and  $\text{NO}_3^-$  as the sole nitrogen source in root tissues.** Top 10 KEGG metabolic pathway enrichments ( $P < .05$ , hypergeometric test) in up-regulated (A) and

950 down-regulated (B) differentially expressed genes in roots from Gene Atlas plants in ammonia vs. nitrate comparison. 'gene.ratio'  
951 represents the ratio of number of DEGs over the number of genes annotated specific to the pathway.